J Biomol NMR (2007) 37:205–224
DOI 10.1007/s10858-006-9128-4

ARTICLE

Improved pulse sequences for sequence specific assignment of aromatic proton resonances in proteins

Frank Löhr · Robert Hänsel · Vladimir V. Rogov · Volker Dötsch

Received: 8 August 2006 / Accepted: 23 November 2006 / Published online: 20 January 2007

Abstract Aromatic proton resonances of proteins are notoriously difficult to assign. Through-bond correlation experiments are preferable over experiments that rely on through-space interactions because they permit aromatic chemical shift assignments to be established independently of the structure determination process. Known experimental schemes involving a magnetization transfer across the C^{β}–C^{γ} bond in aromatic side chains either suffer from low efficiency for the relay beyond the C^{δ} position, use sophisticated ^{13}C mixing schemes, require probe heads suitable for application of high ^{13}C radio-frequency fields or rely on specialized isotopic labelling patterns. Novel methods are proposed that result in sequential assignment of all aromatic protons in uniformly $^{13}C/^{15}N$ labelled proteins using standard spectrometer hardware. Pulse sequences consist of routinely used building blocks and are therefore reasonably simple to implement. Ring protons may be correlated with β-carbons and, alternatively, with amide protons (and nitrogens) or carbonyls in order to take advantage of the superior dispersion of backbone resonances. It is possible to record spectra in a non-selective manner, yielding signals of all aromatic residues, or as amino-acid type selective versions to further reduce ambiguities. The new experiments are demonstrated with four different proteins with molecular weights ranging from 11 kDa to 23 kDa. Their performance is compared with that of (Hβ)Cβ(CγCδ)Hδ and (Hβ)Cβ(CγCδCε)Hε pulse sequences [Yamazaki et al. (1993) J Am Chem Soc 115:11054–11055].

Keywords Amino-acid type selectivity · CC-TOCSY · Direct carbon detection · Heteronuclear cross-polarization · Strong coupling · Triple-resonance NMR

Introduction

Aromatic amino acid residues play a significant role in the architecture of the hydrophobic core of many proteins. Their ring proton resonances are therefore involved in many long-range NOE contacts, rendering their assignment essential for determining the protein's solution structure at high accuracy. Contrary to their aliphatic counterparts, the sequence specific assignment of aromatic side chains cannot be achieved by ^{1}H–^{1}H *J*-correlated experiments as the scalar coupling network is interrupted by the quarternary carbon at the γ position (Wüthrich et al. 1986). Likewise, standard heteronuclear experiments such as HCCH-TOCSY (Bax et al. 1990) or or HC(CCO)NH-TOCSY (Montelione et al. 1992; Logan et al. 1993; Grzesiek et al. 1993) usually fail because of the large offset between aliphatic and aromatic carbon resonances, although it has been shown that the transfer between the two ^{13}C species can be achieved with a HCCH-TOCSY sequence using a microcoil flow-through

Electronic Supplementary Material The online version of this article (doi: 10.1007/s10858-006-9128-4) contains supplementary material, which is available to authorized users.

F. Löhr (✉) · R. Hänsel · V. V. Rogov · V. Dötsch
Institute of Biophysical Chemistry, Centre for Biomolecular Magnetic Resonance, Johann Wolfgang Goethe-University, Frankfurt am Main, Biozentrum N230, 1. OG, Max-von-Laue-Strasse 9, 60438 Frankfurt, Germany
e-mail: murph@bpc.uni-frankfurt.de

probe which allows for the application of very high ^{13}C spin-lock fields (Peti et al. 2004). The 'classical' solution involves linking aromatic protons to previously assigned α- or β-protons (Wagner and Wüthrich 1982; Billeter et al. 1982; Wüthrich 1986) or, as recently suggested, to amide protons (Lin et al. 2006) via intraresidual and sequential NOE connectivities. Although this strategy has been successfully applied in many cases, through-space interactions are not always unambiguous, especially if multiple aromatic rings are in close proximity. With increasing size of the protein complete assignments become more difficult to obtain because of high densities of NOE cross peaks or a poor dispersion of aromatic ^{1}H chemical shifts.

Using a a promising new approach, NOEs involving unassigned aromatic resonances can still be employed to generate distance constraints and finally lead to correct assignments (AB et al. 2006). Nevertheless, to minimize the possibility of introducing consistent but false constraints it is desirable to separate the resonance assignment process from the evaluation of NOESY spectra, suggesting to exclusively make use of scalar couplings for sequence-specific assignment. This was accomplished in a pioneering work by Yamazaki et al. (1993), who developed (Hβ)Cβ(CγCδ)Hδ and (Hβ)Cβ(CγCδCε)Hε experiments giving rise to $^{13}C^{\beta}$–$^{1}H^{\delta}$ and $^{13}C^{\beta}$–$^{1}H^{\varepsilon}$ correlations, respectively, in aromatic side chains. These pulse schemes employ multiple ^{13}C–^{13}C COSY transfer steps to relay magnetization from the originating β-carbon to the destination aromatic carbon. While the (Hβ)Cβ(CγCδ)Hδ sequence usually affords the desired $^{1}H^{\delta}$ assignments for all aromatic amino acid types, introduction of the $^{13}C^{\delta} \rightarrow {}^{13}C^{\varepsilon}$ transfer to obtain additional $^{1}H^{\varepsilon}$ assignments of phenylalanine and tyrosine rings comes at the cost of reduced sensitivity. The (Hβ)Cβ(CγCδCε)Hε experiment becomes particularly critical for phenylalanine residues subject to strong coupling effects due to small chemical shift differences of aromatic ^{13}C nuclei in combination with relatively large $^{1}J_{CC}$ couplings. The transfer efficiency is even more degraded by insertion of a further CC-COSY module aiming at the detection of $^{13}C^{\beta}$–$^{1}H^{\zeta}$ correlations. In an elegant manner, the complete assignment of phenylalanine ring protons was achieved in the AMNESIA sequence (Grzesiek and Bax 1995), in which all CC-COSY elements are replaced by a single Hartmann–Hahn-type transfer, intentionally removing ^{13}C chemical shift differences. Efficient cross polarization over the wide range spanned by $^{13}C^{\beta}$ and aromatic ^{13}C chemical shifts was accomplished via audio modulation of the applied RF field. A related experiment, (HB)CB(CCaro)H (Carlomagno et al. 1996), employs a PLUSH TACSY element for the $^{13}C^{\beta} \rightarrow {}^{3}C^{\gamma}$ transfer followed by homonuclear isotropic mixing for further transfer within aromatic rings. Due to their sophisticated carbon–carbon mixing schemes, implementation of the latter two pulse sequences is, however, not straightforward. Presumably for this reason (Hβ)Cβ(CγCδ)Hδ/Hβ)Cβ(CγCδCε)Hε experiments are usually preferred and are now established standard tools for the sequential assignment of aromatic resonances although improvements afforded by AMNESIA or (HB)CB(CCaro)H sequences in the case of phenylalanine residues have been clearly demonstrated.

Powerful new pulse sequences, HBCB(CG)HE and HBCB(CGCZ)HZ, were recently described to obtain correlations of tyrosine and phenylalanine ε-protons and of phenylalanine ζ-protons with β-$^{13}C/^{1}H/^{2}H$ methylene groups (Torizawa et al. 2005). They rely on long-range $^{13}C^{\gamma}$–$^{1}H^{\varepsilon}$ and $^{13}C^{\gamma}$—$^{13}C^{\zeta}$ couplings, respectively, for the crucial transfer step within the aromatic rings. As a drawback these methods are not applicable to uniformly or randomly labelled proteins. Instead, regioselectively [$^{1}H^{\beta}$–$^{13}C^{\beta}$–$^{13}C^{\gamma}$–$^{13}C^{\varepsilon}$–$^{1}H^{\varepsilon}$]- and [$^{1}H^{\beta}$–$^{13}C^{\beta}$–$^{13}C^{\gamma}$–$^{13}C^{\zeta}$–$^{1}H^{\zeta}$]-labelled amino acids are required in which other nonexchangeable hydrogens are replaced with deuterons in order to avoid strong coupling effects, exclude competing magnetization transfer pathways and minimize dipolar interactions responsible for transverse relaxation. Such amino acids may not be readily available and can only be incorporated economically with the help of cell-free expression systems.

Here we propose an alternative (H)CB(CGCC-TOCSY)H^{ar} experiment suitable for uniformly $^{13}C/^{15}N$-labelled proteins which comprises only standard pulse sequence elements and is therefore comparatively easy to implement. It combines a $^{13}C^{\beta}$, $^{13}C^{\gamma}$ COSY step with a regular homonuclear isotropic mixing scheme to relay ^{13}C magnetization to other aromatic sites as in previous approaches to aromatic resonance assignment (Carlomagno et al. 1996; Löhr et al. 1996; Prompers et al. 1998). Since methods dedicated to the sequence specific assignment of histidine and tryptophan ring resonances have been described previously (Löhr et al. 2002, 2005; Schlörb et al. 2005) the focus in this study will be on phenylalanine and tyrosine residues, but the new pulse scheme may be useful for the former residue types, too, as will be demonstrated for specific cases.

Similar to other sequences (Yamazaki et al. 1993; Grzesiek and Bax 1995; Carlomagno et al. 1996) the (H)CB(CGCC-TOCSY)H^{ar} experiment relies on side chain-to-side chain correlations involving β-carbons. In the case of degenerate $^{13}C^{\beta}$ chemical shifts the

sequence specific assignment of aromatic resonances therefore remains ambiguous. An obvious solution would be additional sampling of β-proton chemical shifts (Löhr et al. 1996; Prompers et al. 1998; Torizawa et al. 2005). The disadvantages of this approach is the concomitant loss of sensitivity resulting from the higher dimensionality and the division of signal intensity on two separate cross peaks unless stereospecific deuteration at the β-methylene group is employed (Torizawa et al. 2005). As will be shown, some simplification of the basic two-dimensional $^{13}C^{\beta}$–$^{1}H^{ar}$ spectra can be achieved by use of band-selective ^{13}C pulses, exploiting the characteristic $^{13}C^{\gamma}$ frequency regions of individual aromatic amino acid types (Schubert et al. 2001; Torizawa et al. 2005). Considerably higher resolution can be gained with an extension of the novel pulse scheme to provide direct correlations between aromatic proton and backbone $^{1}H^{N}/^{15}N$ resonances. Such a H^{ar}(CC-TOCSY-CGCBCAC-O)NH experiment allows sequence specific assignments of ring protons to be obtained without prior knowledge of β-carbon/proton chemical shifts. Conversely, it might be useful in the course of the sequential backbone assignment process, indicating which signals in the ^{15}N,^{1}H-correlation map originate from residues sequentially following aromatic residues.

On the other hand, there are situations where amide protons are not detectable, limiting the applicability of the H^{ar}(CC-TOCSY-CGCBCACO)NH experiment. Possible reasons might be that the labelled protein has been prepared in D_2O-based buffer in order to acquire ^{13}C-resolved NOESY data or that amide proton resonances are broadened due to conformational exchange or rapid chemical exchange with the solvent. Also, aromatic residues may be sequentially followed by a proline. Following a strategy already successfully applied to the assignment of backbone and aliphatic side-chain carbon resonances in deuterated or paramagnetic proteins where protons are either sparse or subject to fast transverse relaxation (Oh et al. 1988; Bertini et al. 2001, 2004a, b; Machonkin et al. 2002, 2004; Kostic et al. 2002; Bermel et al. 2003; Pervushin and Eletsky 2003; Eletsky et al. 2003) an alternative ^{13}C-detected version, HC^{ar}(CC-TOCSY-CGCBCA)-CO, represents a possible remedy.

Materials and methods

Description of the pulse sequences

Each of the three new experiments proposed in this contribution exclusively employ one-bond scalar couplings to correlate aromatic protons with either β-carbons, amide protons and nitrogens or directly attached aromatic carbons and carbonyls. However, as indicated in Fig. 1, the flow of magnetization proceeds in different directions. The (H)CB(CGCC-TOCSY)H^{ar} experiment depicted in Fig. 2 is based on the (Hβ)Cβ(CγCδ)Hδ/(Hβ)Cβ(CγCδCε)Hε pulse sequence pair (Yamazaki et al. 1993). A minor difference involves the implementation of the constant-time $^{13}C^{\beta}$ chemical shift evolution period T_C during which antiphase coherence with respect to $^{13}C^{\gamma}$ builds up.

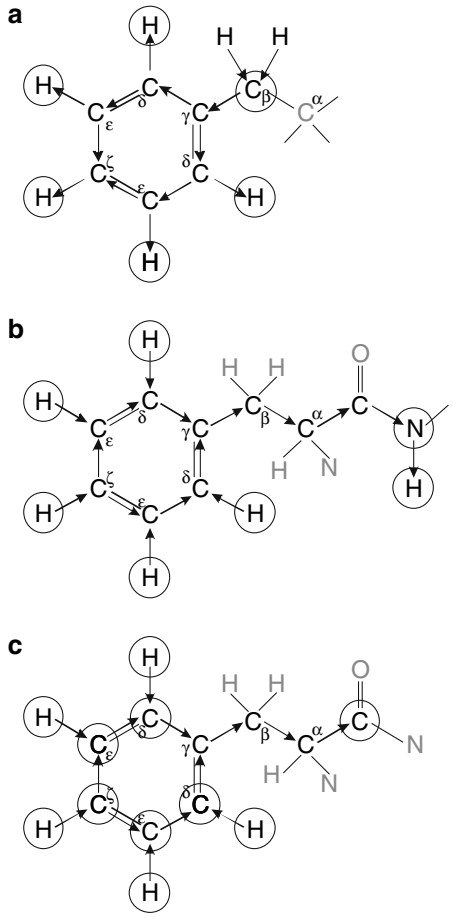

Fig. 1 Schematic drawing of the correlations obtained in (**a**) (H)CB(CGCC-TOCSY)H^{ar}, (**b**) H^{ar}(CC-TOCSY-CGCBCAC-O)NH and (**c**) HC^{ar}(CC-TOCSY-CGCBCA)CO experiments. Chemical shifts of circled nuclei are recorded. Arrows indicate the flow of magnetization along the one-bond coupling network in a phenylalanine residue as an example. In tyrosine residues, the ζ-carbon has a hydroxyl substituent such that the magnetization is not passed beyond the ε-position. See text for peculiarities in aromatic rings of tryptophan and histidine residues. In all experiments, CC-TOCSY is employed for mixing within the rings systems. Coherence transfer between aromatic protons and carbons in (**a**) and (**b**) is achieved with heteronuclear cross polarization and with INEPT in (**c**). CC-COSY and INEPT modules account for the remaining transfer steps, including the $^{13}C^{\beta}$–$^{13}C^{\gamma}$ link

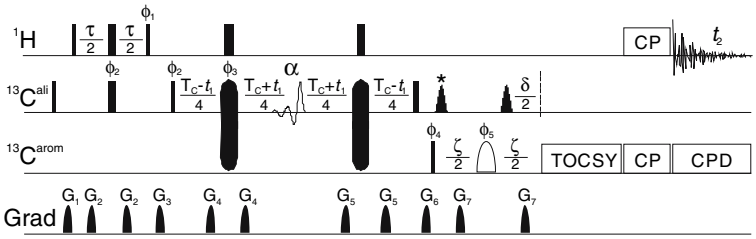

Fig. 2 Two-dimensional (H)CB(CGCC-TOCSY)H^{ar} pulse scheme for detection of connectivities between β-carbons and ring protons in aromatic side chains. Narrow and wide filled bars denote rectangular 90° and 180° pulses, respectively. Pulse widths given in the following are suitable for application at 500 MHz ^{1}H frequency. The proton carrier is positioned at the water resonance throughout the sequence and ^{1}H pulses are applied with the highest available power. Pulses on aliphatic and aromatic carbons are centred at 40.5 ppm and 132.2 ppm, respectively, with the exception of the 2.5-ms I-BURP-2 (Geen and Freeman 1991) pulse labelled α which is applied at an offset of 59 ppm using phase modulation (Boyd and Soffe 1989; Patt 1992). The initial ^{13}C 90° and 180° pulses employ an RF field of about 20 kHz. For the remaining 90° pulses the RF field is reduced to $\Delta/\sqrt{15}$, where Δ is the difference (in Hz) between the aliphatic and aromatic carrier positions. The long filled bars with rounded corners denote 500-μs WURST-20 (Kupče et al. 1995) pulses (80 kHz sweep) that are centred in the aliphatic region but invert aromatic carbon spins, too. The 180° ^{13}C pulse in the centre of the ζ interval is a G^3 Gaussian cascade (Emsley and Bodenhausen 1990) with a duration of 350 μs in the non-selective version of the experiment. A 4-ms RE-BURP (Geen and Freeman 1991) pulse applied at 141, 129 and 111 ppm, respectively, is employed for Phe-, Tyr- and Trp-selective versions. Phase modulated 180° pulses on $^{13}C^{\beta}$ in the same period have the shape of the centre lobe of a sinc-function and a width of 150 μs, where the first one (labelled with an asterisk) is inserted to compensate Bloch-Siegert-like phase shifts. Carbon composite pulse decoupling (CPD) during acquisition is accomplished by GARP-1 modulation (Shaka et al. 1985) with a 1.7-kHz RF field. The ^{13}C TOCSY period consists of one cycle of DIPSI-2 (Shaka et al. 1988) at an RF field strength of 3.3 kHz, corresponding to a mixing time of 8.6 ms (see text for modifications required to additionally detect aromatic resonances beyond $^1H^{\delta}$ in tryptophan and histidine). For the following ^{13}C–^{1}H cross-polarization (CP) transfer, which also employs a single DIPSI-2 cycle, the RF field is increased to 5.4 kHz, such that the duration becomes 5.3 ms ($\approx 1/^1J_{CHarom}$). Both CP and TOCSY sequences are applied along the x-axis. Delay durations in the non-selective version are τ = 3.4 ms ($\approx 1/(2^1J_{CHali})$), T_C = 9 ms (including the duration of the $^{13}C^{\alpha}$-selective pulse) (= $5/(4^1J_{CHali})$ [$1/(2^1J_{C\beta C\gamma}$; ζ = 17.4 *ms*($\approx 1/^1J_{C\gamma C\delta}$); δ = 10.4 *ms*($\approx 1/(2^1J_{C\beta C\gamma})$). The duration ζ (not including the $^{13}C^{\gamma}$-selective 180° pulse in its centre) is reduced to 10.6 ms in the Phe- and Trp-selective versions and to 14 ms in the Tyr-selective version. All gradients are sine-bell shaped and are applied along the z-axis. Their duration is 0.5 ms, except for G_4 and G_5, which have a duration of 0.1 ms. Peak amplitudes of $G_{1,2,3,4,5,6,7}$ are 6, 5, 7.5, 7.5, 5.5, 10, 6.5 G/cm. Unless specified, pulses are applied along the x-axis. Phase cycling is: φ_1 = y, –y; φ_2 = 2(x), 2(–x); φ_3 = 8(x), 8(–x), 8(y), 8(–y); φ_4 = 8(x), 8(–x); φ_5 = 2(x), 2(–x), 2(y), 2(–y); receiver = R, 2(–R), R, where R = x, 2(–x), x, –x, 2(x), –x. Quadrature detection in t_1 is achieved by altering φ_2 in the States-TPPI (Marion et al. 1989) manner

The original (Hβ)Cβ(CγCδ)Hδ/(Hβ)Cβ(CγCδCε)Hε scheme employs separate pulses for inversion and refocusing of aromatic and aliphatic carbon magnetization, the latter consisting of a pair of 90° pulses separated by $1/(2\Delta)$–$(4/\pi)\tau_{90}$, where Δ is the offset between $^{13}C^{\beta}$ and $^{13}C^{\alpha}$ resonance frequencies and τ_{90} is the pulse width. When applied at the centre of T_C this ensures removal of the passive $^1J_{C\alpha C\beta}$ interaction. Shifting the refocusing pulse as a function of t_1 however gradually reintroduces the coupling leading to line-broadening along the $^{13}C^{\beta}$ dimension. This undesired effect is avoided here by means of a $^{13}C^{\alpha}$ elective decoupling pulse, fixed at $T_C/2$, in combination with a pair of adiabatic inversion pulses, initially applied at $T_C/4$ and $3T_C/4$, that cover both the aliphatic and aromatic chemical shift regions such that the $^1J_{C\beta C\gamma}$ coupling is active throughout T_C. Moving these pulse in opposite directions as a function of t_1 causes $^{13}C^{\beta}$ chemical shift evolution while eliminating the $^1J_{C\alpha C\beta}$ coupling at any time. Their arrangement in a double pulsed field gradient spin-echo (DPFGSE) prevents phase distortions in the ^{13}C dimension. Since the timing of ^{13}C pulses is not compatible with proton composite pulse decoupling (CPD) after a fixed period of $1/(4^1J_{C\beta H\beta})$, the T_C period is adjusted to $5/(4\ ^1J_{C\beta H\beta})$, somewhat shorter than $1/(2\ ^1J_{C\beta C\gamma})$], and ^{1}H 180° pulses are applied simultaneously with the adiabatic ^{13}C pulses, allowing for refocusing of the heteronuclear coupling at the end of T_C. For better comparison with the novel method the pulse sequences employed to record reference (Hβ)Cβ(CγCδ)Hδ and (Hβ)Cβ(CγCδCε)Hε spectra adopt this modification, resulting in the same resolution in the indirectly detected dimension. The pulse schemes for the these slightly modified ''Yamazaki-type'' experiments are given in the Supplementary Material (Fig. S1). A (Hβ)Cβ(CγCδCεCζ)Hζ sequence is simply constructed by insertion of a second $\xi/2$–180° (^{13}C)-$\xi/2$–90° (^{13}C) interval as in the related CG(CDCECZ)H experiment (Prompers et al. 1998), where magnetization transfer originates at γ-carbons.

After the polarization transfer from β- to γ-carbons in the (H)CB(CGCC-TOCSY)H^{ar} pulse sequence

in-phase ^{13}C magnetization is relayed to ring protons using isotropic mixing (Fesik et al. 1990; Bax et al. 1990) followed by heteronuclear cross-polarization (CP) (Bearden and Brown 1989; Zuiderweg 1990; Ernst et al. 1991). This requires complete refocusing of the $^{13}C^{\beta}$–$^{13}C^{\gamma}$ coupling as well as suppression of couplings involving the two adjacent ring carbons, which is easily achieved by adjusting the delays δ and ζ to $1/(2^1J_{C\beta C\gamma})$ and $1/^1J_{C\gamma C\delta}$, respectively (Prompers et al. 1998). Alternatively, the bandselective G^3-shaped 180° pulse in the centre of the ζ period, covering the entire aromatic region, may be replaced by a $^{13}C^{\gamma}$-selective RE-BURP pulse. Thus amino-acid type selective subspectra can be recorded for tyrosine, phenylalanine and tryptophan residues, which have distinct $^{13}C^{\gamma}$ chemical shift regions, whereas histidine $^{13}C^{\gamma}$ chemical shifts are less specific due to their dependence on pH and tautomeric states. Since the evolution of $^1J_{C\gamma C\delta}$ couplings is refocused in the Phe- and Trp-selective versions, the length of ζ can be reduced to $\leq 1/(2^1J_{C\beta C\gamma})$ $(=\delta)$. For tyrosines, however, the condition $\zeta = 1/^1J_{C\gamma C\delta}$, must be maintained because their γ- and δ-carbons resonate in the same region. Subsequent CC-TOCSY and CH-CP periods each consist of one cycle of DIPSI-2 (Shaka et al. 1988), applied at RF field strengths of 3.3 kHz and 5.4 kHz, respectively. The corresponding duration of the CC mixing period was empirically optimized to achieve approximately uniform cross peak intensities for δ- and ε-protons of tyrosine residues and δ- and ε- and ζ-protons of phenylalanine residues, while the CP time matches $1/^1J_{CHarom}$.

The H^{ar}(CC-TOCSY-CGCBCACO)NH pulse sequence shown in Fig. 3 has been designed to correlate aromatic protons of a residue i directly to backbone amide protons and nitrogens of the sequentially following residues. For histidine and tryptophan residues this has previously been achieved with the help of a related experiment, H(CDCGCBCACO)NH (Löhr et al. 2005). The presence of $^{13}C^{\delta}$–$^{13}C^{\varepsilon}$ scalar couplings and two $^{13}C^{\gamma}$–$^{13}C^{\delta}$ couplings of equal size, however, renders this scheme unsuitable for a transfer of magnetization between the aromatic and aliphatic moieties in tyrosine and phenylalanine side chains. To this end the first part of the H(CDCGCBCACO)NH sequence has been replaced by a time-reversed version of the (H)CB(CGCC-TOCSY)H^{ar} sequence, where the latter one-bond couplings are constructively used for the transfer within the aromatic rings. The second half of the pulse sequence remains to be identical to that of the CBCA(CO)NH experiment (Grzesiek and Bax 1992), supplemented with sensitivity enhancement and gradient coherence selection (Kay et al. 1992; Muhandiram and Kay 1994) in a standard manner, such that the resulting overall pathway is $^1H^{ar}{}_i(t_1)$,$CP \rightarrow {}^{13}C^{ar}{}_i$, CC-TOCSY $\rightarrow {}^{13}C^{\gamma}{}_i \rightarrow {}^{13}C^{\beta}{}_i \rightarrow {}^{13}C^{\alpha}{}_i \rightarrow {}^{13}C'_i \rightarrow {}^{15}N'_{i+1}$ $(t_2) \rightarrow {}^1H^N{}_{i+1}(t_3)$. Concatenation of the two parts involves simultaneous re- and dephasing of $^{13}C^{\beta}$ magnetization with respect to ^1J coupled γ- and α-carbons, respectively, in the interval between the 90° pulses of phases φ_4 and φ_5 (Fig. 3). Therefore, the C^{α}-selective inversion pulse that was required in the centre of the corresponding period in the (H)CB(CGCC-TOCSY)H^{ar} sequence, is omitted here. Since ^{13}C-^1H polarization transfer is not induced at this stage of the sequence, CPD can be applied to protons throughout this delay. As a consequence, fine tuning of δ to match $5/(4\,{}^1J_{C\beta H\beta})$ is no longer necessary, suggesting its adjustment to $\approx 1/(2^1J_{C\beta C\gamma})$, slightly shorter than $1/(2^1J_{C\alpha C\beta})$. Again, non-selective as well as amino-acid type selective spectra can be obtained, depending on the parameter settings involving duration ζ and the 180° $^{13}C^{ar}$ pulse in its centre (see figure legend for details).

Figure 4 presents a truncated version of the H^{ar}(CC-TOCSY-CGCBCACO)NH sequence, where the $^{13}C'_i \rightarrow {}^{15}N'_{i+1}$ and $^{15}N'_{i+1} \rightarrow {}^1H^N_{i+1}$ transfer steps have been omitted. The resulting HC^{ar}(CC-TOCSY-CGCBCA)CO scheme consequently employs direct detection of carbonyl ^{13}C nuclei (Bertini et al. 2001, 2004a,b; Serber et al. 2001; Kostic et al. 2002; Pervushin and Eletsky 2003; Bermel et al. 2003, 2005). In order to eliminate splittings due to the homonuclear $^1J_{C\alpha C'}$ interaction, an IPAP (Ottiger et al. 1998; Andersson et al. 1998) module is inserted prior to acquisition and the separated doublet components are recombined to enhance sensitivity as described by Bermel et al. (2005). As a minor modification, the antiphase subspectrum is recorded with a ε′ period significantly shorter than $1/(2^1J_{C\alpha C'})$ in order to improve the signal-to-noise ratio, while RF pulses and gradients are retained (see figure legend). In the current version the $^1H \rightarrow {}^{13}C$ CP period has been replaced by a refocused INEPT (Burum and Ernst 1980) polarization transfer, incorporating ^1H (t_1) and ^{13}C (t_2) chemical shift evolution in a semi-constant time (Logan et al. 1992; Grzesiek and Bax 1993) manner. Backbone carbonyl resonances are therefore linked to aromatic proton and to the corresponding directly attached carbon resonances of the same residue. The CC-TOCSY sequence should be adjusted to 8.0 ms (one cycle of DIPSI-2 at an RF field of 3.6 kHz), 11.1 ms (two cycles of DIPSI-2, RF field 5.2 kHz) and 15.0 ms (three cycles of DIPSI-2, RF field 5.7 kHz) to obtain optimal results for tyrosine, phenylalanine and tryptophan spin systems, respectively.

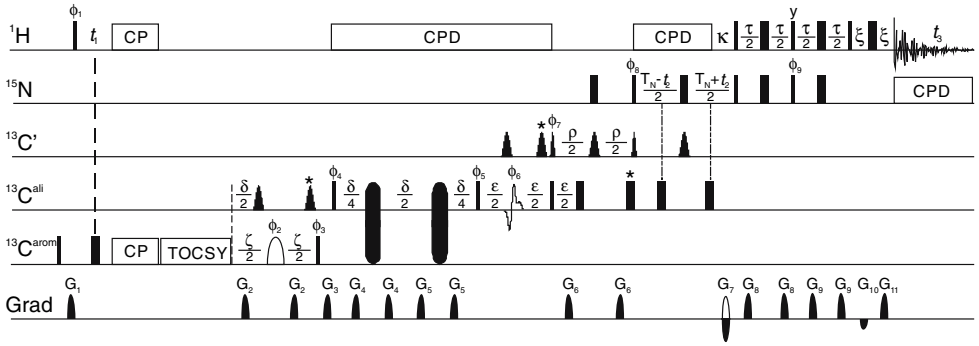

Fig. 3 Three-dimensional H^{ar}(CC-TOCSY-CGCBCACO)NH pulse sequence for obtaining correlations between aromatic protons and backbone amides of sequentially following amino acids. The ^{1}H carrier frequency is placed in the aromatic region (ca. 7 ppm) during t_1 and the following cross-polarization period, then shifted to the $^1H^{\alpha}/^1H^{\beta}$ (ca. 4 ppm) and amide (ca. 8 ppm) regions, respectively, for application of the first and second CPD sequence and finally set to the water resonance for the remainig pulses and acquisition. Proton and nitrogen 90° and 180° pulses are applied with the highest available power while RF field strengths of 4.2 kHz and 0.7 kHz are employed for ^{1}H WALTZ-16 (Shaka et al. 1983) and ^{15}N GARP-1 decoupling. Pulses on nitrogens, carbonyl, aromatic and aliphatic carbons are centred in the amide region (≈117 ppm) and at 176, 132 and 41 ppm, respectively, where the latter two values are optimized for phenylalanine and tyrosine residues, while 124 ppm and 31 ppm are appropriate for tryptophans. Exceptions are the last two 90° and the last four 180° rectangular carbon pulses which are applied at 56 ppm with durations corresponding to RF fields $\Delta/\sqrt{15}$ and $\Delta/\sqrt{3}$, respectively, Δ denoting the difference (in Hz) between the $^{13}C^{\alpha}$ and the carbonyl region. An RF field strength of ca. 20 kHz is used for the initial two ^{13}C pulses. RF fields (durations) are adjusted to 5.4 kHz (5.3 ms) and 3.3 kHz (8.6 ms) for ^{1}H–^{13}C CP and ^{13}C TOCSY DIPSI-2 sequences, respectively, which are both applied along the x-axis. The rectangular 90° pulses with phases φ_3 and φ_4 employ an RF field of $\Delta/\sqrt{15}$, where Δ is recalculated to match the difference between the aromatic and aliphatic carrier positions. The open shape in the centre of period ζ represents a G^3 pulse with a duration of 350 μs in the non-selective version of the experiment. To selectively observe correlations from phenylalanine, tyrosine (+ histidine in some cases) and tryptophan residues the latter pulse is replaced by a 3.5-ms RE-BURP pulse applied at 141, 129 and 111 ppm, respectively. The Trp-selective version employs a 5-kHz RF field for the ^{13}C TOCSY sequence which has a duration of 11.5 ms (corresponding to two cycles of DIPSI-2). Off-resonance 180° pulses on aliphatic carbons during period ζ are sinc-shaped and have a duration of 150 μs. The same shape and duration is used for carbonyl 90° and 180° pulses. Inversion (refocussing) of aromatic (aliphatic) carbon magnetization during period δ is accomplished by 500-μs WURST-20 pulses with an 80-kHz sweep. The shaped pulse on alipatic carbons in the centre of period ε is a 350-μs G^3 Gaussian cascade. Bloch-Siegert compensation pulses are labelled with an asterisk. Delays are adjusted as follows for the non-selective version: ζ = 17.4 ms ($\approx 1/{}^1J_{C_\gamma C_\delta}$); δ = 10.4 ms ($\approx 1/2{}^1J_{C_\beta C_\gamma}$)); ε = 9.2 ms ($\approx 1/(2{}^1J_{C_\alpha C'})$); ρ = 22 ms ([$1/(2{}^1J_{C'N})$); T_N = 25 ms ([$1/(2{}^1J_{C'N})$); κ = 5.4 ms ($\approx 1/(2{}^1J_{NH})$); τ = 4.6 ms ([$1/(2{}^1J_{NH})$); χ = 0.375 ms (duration of G_{10}/G_{11} + recovery time). Delay ζ is shortened to 14 ms in the Tyr-selective version and to 10.6 ms in the Phe- and Trp-selective versions, where the durations do not include the widths of the bandselective 180° $^{13}C^{arom}$ pulse in their centre. Pulsed field gradients have the following durations, peak amplitudes and directions: G_1 = (0.5 ms, 6 G/cm, z), G_2 = (0.5 ms, 7.5 G/cm, x), G_3 = (0.5 ms, 7.5 G/cm, y), G_4 = (0.1 ms, 10 G/cm, x), G_5 = (0.1 ms, 10 G/cm, y), G_6 = (0.5 ms, 6 G/cm, x), G_7 = (1.4 ms, –19.78 G/cm, xyz), G_8 = (0.3 ms, 4 G/cm, xy), G_9 = (0.3 ms, 5.5 G/cm, xy), G_{10} = (0.175 ms, –2.5 G/cm, xyz), G_{11} = (0.175 ms, 13.5 G/cm, xyz). Proton CPD is interrupted during application of gradients G_4 and G_5. The default pulse phase is x. Labelled pulse phases are cycled according to: $\varphi_1 = 4(y), 4(-y)$; $\varphi_2 = 32(x), 32(y)$; $\varphi_3 = x, -x$; $\varphi_4 = 8(x), 8(-x)$; $\varphi_5 = 4(x), 4(-x)$;$\varphi_6 = 16(x), 16(y)$; $\varphi_7 = 2(x), 2(-x)$; $\varphi_8 = x$; $\varphi_9 = y$; receiver = R, $2(-R)$, R, $-R$, $2(R)$, $-R$, where $R = x, 2(-x), x, -x, 2(x), -x$. Sign discrimination in the t_1 dimension is accomplished by States-TPPI of φ_1. For each t_2 increment, echo- and antiecho coherence transfer pathways are selected alternately by inversion of the polarity of G_7 along with the pulse phase φ_9 and spectra are processed using the enhanced sensitivity method (Cavanagh et al. 1991; Kay et al. 1992). Axial peaks in the ^{15}N dimension are shifted to the edge of the spectrum by incrementing φ_8 and the receiver phase by 180° for each successive value of t_2

Sample preparations

Uniform ^{13}C;^{15}N-labelling of recombinant flavodoxin from *Desulfovibrio vulgaris* was achieved by growing *E. coli* TG1 in M9 medium containing $^{15}NH_4Cl$ as nitrogen source and $^{13}C_6$ glucose as well as $^{13}C_3$ glycerol as carbon sources. Protein expression and purification was performed as described previously (Curley et al. 1991; Knauf et al., 1993). Measurements were carried out on a 1.2-mM sample of oxidized flavodoxin in 10 mM potassium phosphate buffer, pH 7.0, to which 0.02% sodium azide, 50 μg/ml Complete protease inhibitor and 2 mM EDTA had been added.

The preparation of [*U*-^{13}C;^{15}N]-enriched RNase T1 has been described elsewhere (Spitzner et al. 2001). The pH of the sample employed for NMR measurements, which contained 2 mM of the protein, was adjusted to 5.5.

The gene encoding for thioredoxin was cloned into a pET32a vector which was then transformed into

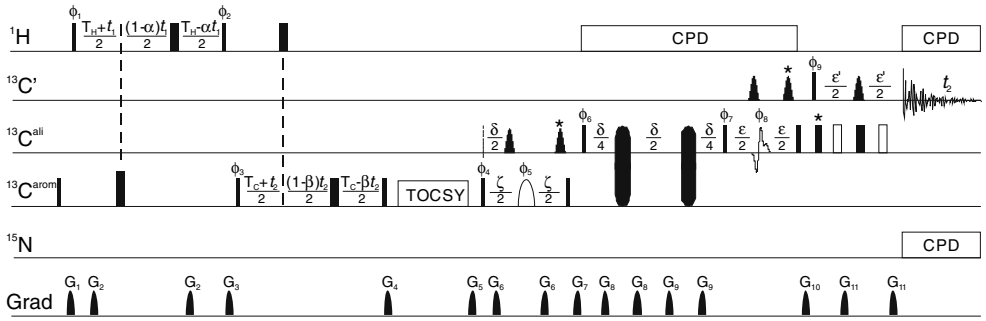

Fig. 4 Pulse sequence of the 3D HC^{ar}(CC-TOCSY-CGCBCA)-CO experiment to correlate carbonyl carbons with intraresidual aromatic carbons and protons. Narrow and wide filled bars denote rectangular 90° and 180° pulses, respectively. The initial four ^{1}H pulses are applied with the highest available power with the carrier frequency placed at 6.9 ppm. Subsequently the carrier position is switched to 4.1 ppm. Proton WALTZ-16 and nitrogen GARP-1 CPD employ RF fields of 4.2 kHz and 0.8 kHz, respectively (RF field strengths and pulse widths given in this figure legend are suitable for application at a 600 MHz spectrometer). Pulses on aromatic, aliphatic and carbonyl carbons are centred at 125.9, 40.1 and 175.6 ppm, respectively, except for the two 90° surrounding the ε period (55 ppm) and the 300–μs G^3 pulse (50 ppm) in its centre. All carbon pulses prior to the TOCSY mixing period (DIPSI-2, RF field 3.6 kHz, duration 8 ms) are applied with an RF field of 16 kHz. The remaining rectangular ^{13}C pulse employ field strengths adjusted to $\Delta/\sqrt{15}$ (90° flip angle) or $\Delta/\sqrt{3}$ (180° flip angle), where Δ denotes the frequency difference between $^{13}C^{\alpha}$ and $^{13}C'$ ($^{13}C^{\beta}$ and $^{13}C^{ar}$ in the case of the three 90° pulses following the TOCSY period). Sinc-shaped 180° pulses with durations of 120 μs are applied to β-carbons (during ζ) and to carbonyl carbons (during ε and ε′). Asterisks indicate Bloch-Siegert compensation pulses. The long solid bars at $\delta/4$ and $3\delta/4$ denote 500-μs WURST-20 pulses (80 kHz sweep) covering aliphatic and aromatic regions. In the non-selective version of the sequence, the 180° $^{13}C^{ar}$ pulse in the centre of ζ has a G^3 shape and a duration of 300 μs. Delays $T_H = T_C(\approx 1/(2^1J_{HCar}))$,$\delta(\approx 1/(2^1J_{C\beta C\gamma}))$, $\zeta(\approx 1/^1J_{C\gamma C\delta}))$ and ε ($\approx 1/J(2^1J_{C\alpha C'})$) have values of 2.78, 10.4, 17.4, and 9.26 ms, respectively. Evolution times t_1 and t_2 are of the semi-constant time type, where parameters α and β are defined by $\alpha = T_H/t_{1max}$ and $\beta = T_C/t_{2max}$. For amino-acid type selective experiments the duration ζ is adjusted to 10.6 ms and the 300-μs G3 pulse in its centre is replaced with a $^{13}C^{\gamma}$-selective 3.3-ms REBURP pulse applied at 141 ppm for phenylalanines and at 111 ppm for tryptophans. Carrier positions for the remaining pulses on aromatic carbons including the TOCSY sequence are placed at 132 ppm and 121 ppm, respectively, in the Phe-and Trp-selective versions. All pulsed field gradients are sine-bell shaped and are applied along the z-axis. Their durations and peak amplitudes are: G_1 = (0.5 ms, 6.5 G/cm), G_2 = (0.1 ms, 9 G/cm), G_3 = (0.5 ms, 7 G/cm), G_4 = (0.5 ms, 6 G/cm), G_5 = (0.5 ms, 4.5 G/cm), G_6 = (0.5 ms, 5.5 G/cm), G_7 = (0.5 ms, 7.5 G/cm), G_8 = (0.1 ms, 7.5 G/cm), G_9 = (0.1 ms, 6.5 G/cm), G_{10} = (0.5 ms, 6.5 G/cm), G_{11} = (0.1 ms, 10 G/cm. Phase cycling is $\varphi_1 = 4(x)$, $4(-x)$; $\varphi_2 = y$; $\varphi_3 = y$, $-y$; $\varphi_4 = 2(y)$, $2(-y)$; $\varphi_5 = 32(x)$, $32(y)$;$\varphi_6 = 8(x)$, $8(-x)$;$\varphi_7 = 4(x)$, $4(-x)$; $\varphi_8 = 16(x)$, $16(y)$; receiver = R, $2(-R)$, R, $-R$, $2(R)$, $-R$ ($R = x$, $2(-x)$, x, $-x$, $2(x)$, $-x$), while unlabelled pulses are applied along x. Quadrature detection in the t_1 and t_2 dimensions is achieved by application of States-TPPI to φ_1 and φ_3, respectively. In-phase and antiphase spectra with respect to $^1J_{C\alpha C'}$ along F_3 are recorded in an interleaved manner. The in-phase subspectrum is obtained when the 180° $^{13}C^{\alpha}$ pulses in the ε′ period (=9.26 ms $\approx 1/(2^1J_{C\alpha C'})$) immediately follow the 90° and 180° pulses on $^{13}C'$, as indicated by the last two filled rectangles, and $\varphi_9 = x$. Shifting the position of the 180° $^{13}C^{\alpha}$ pulses to the centre of each ε′/2 period (indicated by open rectangles) and changing the pulse phase φ_9 to $-y$ results in the antiphase subspectrum. In the latter case the duration of ε′ may be shortened to the minimum time required to accommodate gradients and RF pulses

E.coli BL21(DE3). The bacteria were cultured at 37°C in LB medium and transferred to M9 medium containing 1 g/l $^{15}NH_4Cl$ and 2 g/l $^{13}C_6$ glucose. When the cells had reached an O.D. of 1.0, overexpression of thioredoxin was induced by addition of IPTG to 1 mM and growth was continued overnight. Cells were harvested by centrifugation, resuspended in lysis buffer containing 25 mM histidine, 50 mM NaCl and Complete protease inhibitor mix and disrupted by sonification. Following removal of cell debris by centrifugation, streptomycin was added in order to precipitate DNA. The protein was purified by anion exchange followed by gel filtration chromatography. NMR experiments were performed on the oxidized form of the [U–^{13}C;^{15}N]-labelled protein, which had a concentration of 1.3 mM in 25 mM sodium phosphate buffer at pH 8.5.

Recombinant Family 11 xylanase from *Bacillus agaradhaerens* was expressed in *E. coli* carrying the pET-3a plasmid, encoding for residues 1–207. Growing cells on M9 minimal medium supplemented with 1 g/l $^{13}C_6$ glucose, 2.5 g/l $^{13}C_3$ glycerol and 1 g/l $^{15}NH_4Cl$ yielded [U-^{13}C;^{15}N]-labelled protein. Its purification followed the procedure of Sabini et al. (1999). The sample was dissolved at a concentration of 0.6 mM in 10 mM sodium acetate buffer, pH 5.4, containing 0.03% NaN_3 and 50 μg/ml Pefabloc protease inhibitor.

Flavodoxin, thioredoxin and xylanase samples contained 0.15 mM 3-(trimethylsilyl)-1-propanesulfonic acid (DSS) as internal chemical shift standard and 5% D_2O. They were inserted into Shigemi microcells with volumes ranging from 220 μl to 300 μl. The RNase T1 sample contained 10% D_2O in a volume of 500 μl and was placed in a Wilmad 528-PP NMR tube.

Data acquisition and processing

All proton detected spectra were recorded on a 11.7 T Bruker Avance spectrometer (^{1}H Larmor frequency: 500 MHz) equipped with a 5-mm three-axis gradient ^{1}H{^{13}C, ^{15}N} triple resonance probe. Carbonyl detected experiments were carried out at a 14.1 T Bruker Avance spectrometer (^{1}H Larmor frequency: 600 MHz) using a cryogenic 5-mm z-gradient ^{1}H{^{13}C,^{15}N} triple resonance probe housing cold ^{1}H and ^{13}C preamplifiers. The temperature was maintained at 35, 27, 33 and 35 °C during experiments with RNase T1, flavodoxin, xylanase and thioredoxin, respectively. Acquisition parameters of all experiments are summarized in Table 1. In the non-selective 3D H^{ar}(CC-TOCSY-CGCBCACO)NH experiment on flavodoxin phase cycling of φ_2 has been omitted, allowing to record 32 rather than 64 scans per FID. In the 3D HC^{ar}(CC-TOCSY-CGCBCA)CO experiments FIDs containing in-phase and antiphase signals were collected alternately, each comprising 64 scans.

Spectra processing was performed with the Bruker TopSpin 1.3 software. Typically, time domain data in indirectly detected dimensions were extended by 1/4 to 1/3 of their original length using linear prediction. Prior to zero filling and Fourier transformation squared-cosine weighting functions were applied in all dimensions. Processing of the HC^{ar}(CC-TOCSY-CGCBCA)CO spectrum involved addition and subtraction of the two FIDs stored separately for each increment in order to isolate the two doublet components with respect to $^1J_{CaC'}$. A scaling factor of 0.95 was employed for the antiphase part to account for its slightly higher signal intensities. The two linear combinations were then shifted by $J/2$ in opposite directions and merged to improve the signal-to-noise by a theoretical factor of $2^{1/2}$ (Nielsen et al. 1995; Pervushin and Eletsky 2003; Bermel et al. 2005). Contour levels of all spectra displayed in the following are plotted on an exponential scale with an increment of $2^{1/2}$ allowing for an approximate assessment of the relative sensitivities obtained.

Results and discussion

The key elements of the new methods presented here are the hybrid COSY-TOCSY carbon-carbon mixing followed by carbon–proton cross-polarization to relay magnetization between β-carbons and aromatic protons. The efficiency of this combination may be assessed by comparison of the corresponding (H)CB(CGCC-TOCSY)H^{ar} pulse sequence with the (Hβ)Cβ(CγCδ)Hδ and (Hβ)Cβ(CγCδCε)Hε schemes (Yamazaki et al. 1993), commonly employed to obtain sequence specific assignments of aromatic ^{1}H resonances. The latter exclusively rely on CC-COSY steps for the magnetization transfer along the carbon scaffold of aromatic amino acid side chains and a reverse INEPT for the final polarization transfer to protons. In an effort to observe additional correlations involving phenylalanine ζ-protons a (Hβ)Cβ(CγCδCεCζ)Hζ experiment, derived from the (Hβ)Cβ(CγCδCε)Hε sequence by inserting another CC-COSY step, has been applied as well. While a COSY-type transfer is employed for the $^{13}C^{\beta} \rightarrow {}^{13}C^{\gamma}$ step in either of the sequences, only the (H)CB(CGCC-TOCSY)H^{ar} scheme prevents loss of detectable magnetization due to incomplete rephasing of the $^1J_{C\beta C\gamma}$ coupling and, in the case of spin systems with two equivalent δ-carbon resonances (i.e., phenylalanine and tyrosine), evolution of passive $^1J_{C\gamma C\delta}$ couplings, albeit at the cost of a prolonged duration ζ. Amino-acid type selective versions, in which selective refocusing are applied in the centre of this period, take advantage of the narrow and well-separated $^{13}C^{\gamma}$ chemical shift regions of phenylalanine (≈ 141–137 ppm), tyrosine (≈ 132–127 ppm) and tryptophan (≈ 112–109 ppm) residues, allowing to use ζ delays shorter than $1/^1J_{C\gamma C\delta}$. Note that the corresponding 180° pulse in (Hβ)Cβ(CγCδ)Hδ/(Hβ)Cβ(CγCδCε)Hε experiments must act simultaneously on C$^{\gamma}$ and C$^{\delta}$ spins suggesting a Tyr-selective version as the only option. Using successive homonuclear ^{13}C TOCSY and heteronuclear ^{13}C–^{1}H CP building blocks for the $^{13}C^{\gamma} \rightarrow {}^{13}C^{\delta/\varepsilon/\zeta} \rightarrow {}^{1}H^{\delta/\varepsilon/\zeta}$ pathway the remainder of the (H)CB(CGCC-TOCSY)H^{ar} pulse sequence is void of any pulse-interrupted free-precession periods involving $^{13}C^{\delta}/^{13}C^{\varepsilon}/^{13}C^{\zeta}$. These carbon nuclei are often strongly coupled in phenylalanine spin systems, resulting in inefficient magnetization transfer during (Hβ)Cβ(CγCδCε)Hε and (Hβ)Cβ(CγCδCεCζ)Hζ pulse sequences.

The performance of (Hβ)Cβ(Cγ)Hδ, (Hβ)Cβ(CγCδ-Cε)Hε, (Hβ)Cβ(CγCδCε Cζ)Hζ and (H)CB(CGCC-TOCSY)H^{ar} experiments shall be compared first using the proteins ribonuclease T1 (104 residues) and flavodoxin (147 residues) for which complete resonance assignments are already known. In the (Hβ)Cβ(Cγ-Cδ)Hδ spectrum of RNase T1 (Fig. 5a) intense $^{13}C^{\beta}$–$^1H^{\delta}$ cross peaks are observed for the majority of its phenylalanine and tyrosine residues. However, only a weak correlation can be identified for Tyr56 and none is present for Tyr24, both of which have degenerate $^1H^{\delta}$ and $^1H^{\varepsilon}$ chemical shifts. Correlations for these residues are, however, detected in the (Hβ)-Cβ(CγCδCε)Hε (Fig. 5b). Where $^1H^{\delta}$ and $^1H^{\varepsilon}$ chemical

Table 1 Acquisition parameters employed in the individual experiments for aromatic resonance assignments

Sample	Experiment[a]	Spectral width/ppm (detected nucleus)			Time domain data[b]			Acquisition time/ms			No. scans	Exp. time/h
		F_1	F_2	F_3	t_1	t_2	t_3	t_1	t_2	t_3		
RNase T1	(Hβ)Cβ(CγCδ)Hδ[c]	29.5 (^{13}C$^{\beta}$)	9.0 (^{1}H^{ar})		32	384		8.4	85.4		128	4
	(H)CB(CGCC-TOCSY)H^{ar} [d]	29.5 (^{13}C$^{\beta}$)	9.0(^{1}H^{ar})		32	384		8.4	85.4		128	4
	HC^{ar}(CC-TOCSY-CGCBCA)CO	1.4 (^{1}H^{ar})	21.9 (^{13}C^{ar})	14 (^{13}CO)	15	16	216	17.8	4.8	102.2	64	60
Flavodoxin	(Hβ)Cβ(CγCδ)Hδ[c]	29.5 (^{13}C$^{\beta}$)	9.0 (^{1}H^{ar})		32	384		8.4	85.4		128	4
	(H)CB(CGCC-TOCSY)H^{ar} [d]	29.5 (^{13}C$^{\beta}$)	9.0 (^{1}H^{ar})		32	384		8.4	85.4		128	4
	H^{ar}(CC-TOCSY-CGCBCACO)NH	1.8 (^{1}H^{ar})	30.8 (^{15}N)	12.6 (^{1}H^{N})	26	40	384	28.9	25.0	60.9	32	60
	H^{ar}(CC-TOCSY-CGCBCACO)NH W	2.2 (^{1}H^{ar})	12.0 (^{15}N)	12.6 (^{1}H^{N})	32	16	384	29.0	24.7	60.9	64	60
Xylanase	(Hβ)Cβ(CγCδ)Hδ[c]	29.5 (^{13}C$^{\beta}$)	9.0 (^{1}H^{ar})		32	384		8.4	85.4		640	19
	(H)CB(CGCC-TOCSY)H^{ar} [d]	29.5 (^{13}C$^{\beta}$)	9.0 (^{1}H^{ar})		32	384		8.4	85.4		640	19
	(H^{ar}CC-TOCSY-CGCBCACO)NH[e]	30.8 (^{15}N)	12.6 (^{1}H^{N})		40	352		25.0	55.8		512	22
	H^{ar}(CC-TOCSY-CGCBCACO)NH Y	1.9 (^{1}H^{ar})	30.8 (^{15}N)	12.6 (^{1}H^{N})	12	40	288	12.5	25.0	45.6	128	133
Thioredoxin	(H)CB(CGCC-TOCSY)H^{ar} H	29.5 (^{13}C$^{\beta}$)	9.0 (^{1}H^{ar})		32	384		8.4	85.4		64	2
	HC^{ar}(CC-TOCSY-CGCBCA)CO F	1.5 (^{1}H^{ar})	12.3 (^{13}C^{ar})	14 (^{13}CO)	20	10	216	22.2	5.4	102.2	64	48
	HC^{ar}(CC-TOCSY-CGCBCA)CO W	1.8 (^{1}H^{ar})	28.1 (^{13}C^{ar})	14 (^{13}CO)	22	18	216	20.3	4.2	102.2	64	96

[a] Amino-acid type selective versions are indicated by the one-letter code of the respective aromatic amino acid behind the experiment name

[b] Complex points

[c] Same parameters also used for (Hβ)Cβ(Cγ CδCε)Hε and for (Hβ)Cβ (Cγ CδCε Cζ)Hζ experiments

[d] Non-selective and all amino-acid type selective versions

[e] Two-dimensional amino-acid type selective versions

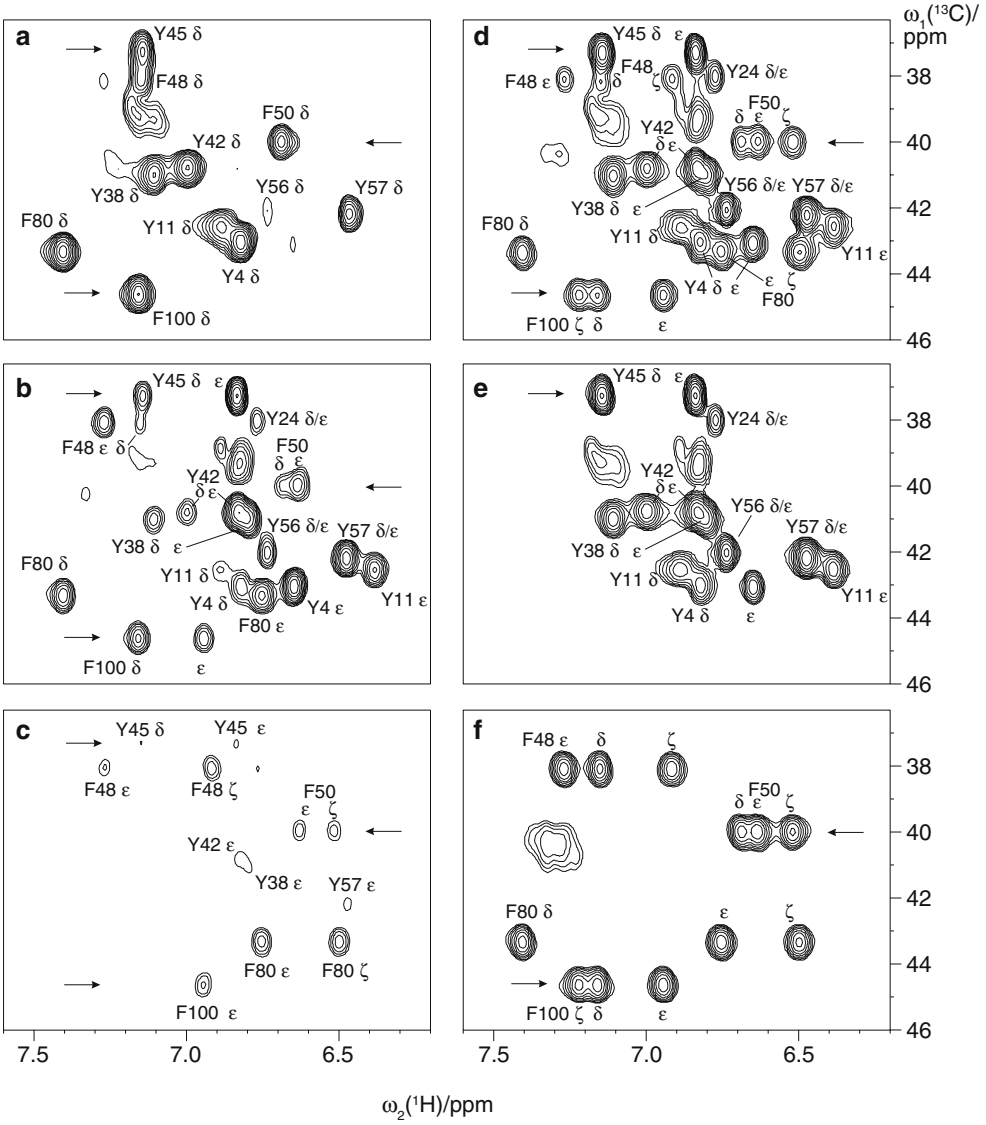

Fig. 5 Regions from (**a**) (Hβ)Cβ(CγCδ)Hδ, (**b**) (Hβ)Cβ(CγCδCε)Hε, (**c**) (Hβ)Cβ(CγCδCεCζ)Hζ, (**d**) non-selective (H)CB(CGCC-TOCSY)H^{ar}, (**e**) Tyr-selective (H)CB(CGCC-TOCSY)H^{ar} and (**f**) Phe-selective (H)CB(CGCC-TOCSY)H^{ar} spectra of RNase T1, containing correlations between β-carbon and aromatic proton resonances of phenylalanine and tyrosine residues. All spectra were recorded under the same experimental conditions, processed in an identical manner and plotted at identical contour levels. Unassigned signals arise from a small fraction of denatured protein in the sample. Residues Tyr24, Tyr56 and Tyr57 have degenerate $^{1}H^{\delta}$ and $^{1}H^{\varepsilon}$ chemical shifts (Hoffmann and Rüterjans 1988). Arrows indicate the positions at which the F_2 traces shown in Fig. 6 are taken

shifts are resolved, $^{13}C^{\beta}$–$^{1}H^{\varepsilon}$ cross peaks are usually stronger than the corresponding $^{13}C^{\beta}$–$^{1}H^{\delta}$ cross peaks in this spectrum. A remarkable exception is Phe100, whose $^{13}C^{\beta}$–$^{1}H^{\delta}$ cross peak is stronger, showing that a distinction based on relative signal intensities may be ambiguous if a (Hβ)Cβ(Cγ CδCε)Hε experiment is performed only. The diminished transfer efficiency to the ε-position in the aromatic ring of Phe100 is most likely caused by the strong coupling between its $^{13}C^{\varepsilon}$ and $^{13}C^{\zeta}$ spins whose resonance frequencies differ by only 0.3 ppm, i.e., less than the scalar coupling constant between the two nuclei. For the same reason the attempt to transfer magnetization via the ζ-carbon failed for this residue and only a $^{13}C^{\beta}$–$^{1}H^{\varepsilon}$ correlation is observed in the (Hβ)Cβ(CγCδCε Cζ)Hζ spectrum (Fig. 5c). The remaining three phenylalanine residues of RNase T1 give rise to relatively weak $^{13}C^{\beta}$–$^{1}H^{\varepsilon}$ and $^{13}C^{\beta}$–$^{1}H^{\zeta}$ correlations, while very weak signals are obtained for some of its tyrosines.

Application of the new (H)CB(CGCC-TOCSY)H^{ar} pulse sequence to RNase T1 resulted in the spectrum shown in Fig. 5d. It contains all expected correlations, including those of residues Tyr24, Tyr56 and Phe100, such that the complete assignment of all aromatic phenylalanine and tyrosine ^{1}H resonances is possible in a single experiment. Notably, the CC-TOCSY mixing time required to transfer magnetization from the γ-carbon to the ζ-carbon is as short as 8.6 ms, limiting the decay due to transverse relaxation. However, it should be mentioned that, not undesirably, ^{13}C–^{13}C as well as ^{1}H–^{1}H homonuclear mixing proceeding during the heteronuclear cross-polarization period also contribute to this transfer. Application of an alternative (H)CB(CGCC-TOCSY)H^{ar} scheme with a ^{13}C–^{1}H

reverse INEPT substituting for the CP element resulted in slightly inferior overall sensitivity and a less uniform distribution of signal intensities within the individual positions of the aromatic rings. Although not a serious problem for RNase T1, signal overlap in (H)CB(CGCC-TOCSY)H^{ar} spectra can be reduced by use of its amino-acid type selective versions. This becomes apparent from Fig. 5e and f which show well-resolved Tyr and Phe subspectra void of spurious signals from the respective other amino acid type.

Relative sensitivities of the various $^{13}C^{\beta}$–$^{1}H^{arom}$ correlation experiments of Fig. 5 can be assessed from traces along the proton dimension taken at well resolved β-carbon resonance positions (Fig. 6). High signal intensities are universally obtained with the shortest pulse sequence, (Hβ)Cβ(CγCδ)Hδ, where the detectable magnetization is confined to δ-protons rather than being shared among several aromatic proton spins as in the remaining experiments. Surprisingly, an even more intense $^{1}H^{\varepsilon}$ cross peak is observed for the Tyr45 in the (Hβ)Cβ(CγCδCε)Hε spectrum whereas peak heights are significantly reduced for both Phe50 and Phe100. A severe loss of sensitivity is evident in the (Hβ)Cβ(CγCδCεCζ)Hζ spectrum which shows only weak signals with one of the targeted $^{13}C^{\beta}$–$^{1}H^{\zeta}$ correlations missing, as noted above. In contrast, the non-selective (H)CB(CGCC-TOCSY)H^{ar} spectrum displays quite uniform and high intensities of $^{1}H^{\delta}$, $^{1}H^{\varepsilon}$ and $^{1}H^{\zeta}$ cross peaks albeit slightly lower than that of individual peaks in (Hβ)Cβ(CγCδ)Hδ or (Hβ)Cβ(CγCδCε)Hε spectra. The increased signal-to-noise ratios in the selective versions of the (H)CB(CGCC-TOCSY)H^{ar} experiment are a consequence of the shorter ζ delays and the refocusing of passive $^{2}J_{C\gamma C\varepsilon}$ and $^{3}J_{C\gamma C\zeta}$ couplings owing to the use of $^{13}C^{\gamma}$ and $^{13}C^{\gamma\delta}$ selective 180° pulses in the case of phenylalanine and tyrosine, respectively.

A similar set of spectra as for RNase T1 was also recorded on *D. vulgaris* flavodoxin featuring a somewhat slower rotational tumbling rate due to its higher molecular weight (16 kDa versus 11 kDa) in combination with the lower temperature (27° vs. 35 °C) during data acquisition, and a lower sample concentration (1.2 mM vs. 2 mM). Spectra are shown in the Supplementary Material (Fig. S2). Using identical measurement times of 4 h per spectrum, adequate signal-to-noise ratios were however obtained in all experiments except for the (Hβ)Cβ(CγCδCεCζ)Hζ which gave rise to useful $^{13}C^{\beta}$–$^{1}H^{\zeta}$ correlations for three of the six phenylalanine residues of flavodoxin only. In each of those (Phe47, Phe71, Phe91) all aromatic ^{13}C resonances are separated by more than 1 ppm whereas in the remaining three residues (Phe50, Phe75, Phe101), $^{13}C^{\delta}$ and $^{13}C^{\varepsilon}$ chemical shifts differ by only 0.8 ppm or less, degrading the performance of (Hβ)Cβ(CγCδCε)Hε and (Hβ)Cβ(CγCδCεCζ)Hζ experiments. By contrast, the (H)CB(CGCC-TOCSY)H^{ar} experiment provides intense cross peaks for all

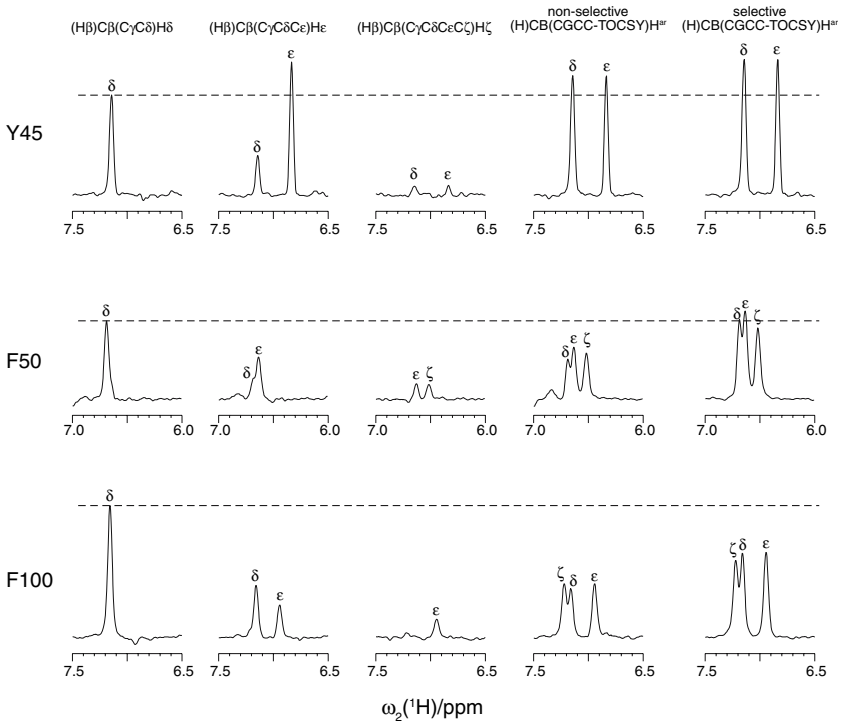

Fig. 6 One-dimensional traces along the F_2 dimensions of the spectra shown in Fig. 5, taken at the $^{13}C^{\beta}$ chemical shifts of Tyr45, Phe50 and Phe100. All ^{1}H traces are plotted with the same vertical scaling. Dashed horizontal lines are drawn at the height of the $^{1}H^{\delta}$ cross peaks in the (Hβ)Cβ(CγCδ)Hδ spectrum

three aromatic protons in all phenylalanine spin systems.

Although the 2D $^{13}C^{\beta}$–$^{1}H^{ar}$ correlation spectra of flavodoxin are not excessively crowded, signal overlap prevents complete aromatic proton assignment. For instance, Tyr31 $^{1}H^{\delta}$, Phe91 $^{1}H^{\varepsilon}$ and Phe101 $^{1}H^{\zeta}$ resonances cannot be identified in the non-selective (H)CB(CGCC-TOCSY)H^{ar} spectrum. A partial solution lies in the application of amino-acid type selective versions, resulting in the separation of the coincident Tyr31 $^{13}C^{\beta}$–$^{1}H^{\delta}$ and Phe101 $^{13}C^{\beta}$–$^{1}H^{\zeta}$ cross peaks (see panels e and f of Fig. S2). However, where $^{13}C^{\beta}$ resonances of two residues of the same type are nearly degenerate, as in the cases of Tyr31/Tyr98 and Phe71/Phe91, the sequence specific assignment of aromatic protons remains ambiguous. The same difficulty applies to the assignment of indole protons of the two tryptophan residues of flavodoxin from a 2D (H)CB(CGCC-TOCSY)H^{ar} spectrum recorded with ^{13}C pulse offsets optimized for tryptophan spins systems and a CC-TOCSY period of 11.5 ms. The longer mixing time allows for a transfer magnetization across the quarternary δ2- and ε2-carbons and thus a detection of protons in the benzene moiety of the indole ring system. A clear distinction as to which of the tryptophan residues the observed ^{1}H resonances belong is hardly possible because the corresponding $^{13}C^{\beta}$ chemical shifts are very similar (see panel g of Fig. S2).

Problems caused by the limited dispersion of $^{13}C^{\beta}$ nuclei may be solved by the usually superior resolution of backbone amide chemical shifts. This has long been exploited in HCC(CO)NH-TOCSY experiments (Montelione et al. 1992; Logan et al. 1993; Grzesiek et al. 1993) which disentangle the crowded aliphatic ^{1}H–^{13}C region via through-bond correlations with the ^{15}N and $^{1}H^{N}$ resonances of the sequentially following residue. An analogous scheme for aromatic residues has not been proposed so far. It is however feasible by taking advantage of the high efficiency of the (H)CB(CGCC-TOCSY)H^{ar} pulse scheme which can also be applied with its direction of magnetization transfer reversed. Appending a standard module to relay magnetization from β-carbons to amide protons across the peptide bond results in the H^{ar}(CC-TOCSY-CGCBCACO)NH sequence. Its utility to lift the ambiguities in the (Hβ)Cβ(CγCδCε)Hε or (H)CB-(CGCC-TOCSY)H^{ar} spectra of flavodoxin is illustrated in Fig. 7. It shows representative $^{1}H^{ar}$–$^{1}H^{N}$ strips of a non-selective and a Trp-selective version of the 3D H^{ar}(CC-TOCSY-CGCBCACO)NH experiment. It should be noted that the increased dimensionality compared to (H)CB(CGCC-TOCSY)H^{ar} does not entail a loss of sensitivity because of of the constant-time nature of the ^{15}N chemical shift evolution and the echo/antiecho type quadrature detection. Previously ambiguous correlations involving the pairs Tyr31/Tyr98 and Trp60/Trp140 appear at different $^{1}H^{N}$ and ^{15}N chemical shifts along the F_2 and F_3 dimensions permitting their sequence-specific assignment. In addition, for the first time a cross peak for Phe91 $^{1}H^{\varepsilon}$ can be discerned, revealing that it was hidden under the intense $^{1}H^{ar}$–$^{13}C^{\beta}$ cluster of Phe71 in either (Hβ)Cβ(CγCδCε)Hε or (H)CB(CGCC-TOCSY)H^{ar} spectra.

Histidine residues frequently occur at the active site of enzymes. Their imidazole ring proton chemical shifts are potential reporters of its protonation state. While (Hβ)Cβ(CγCδ)Hδ and (Hβ)Cβ(CγCδCε)Hε

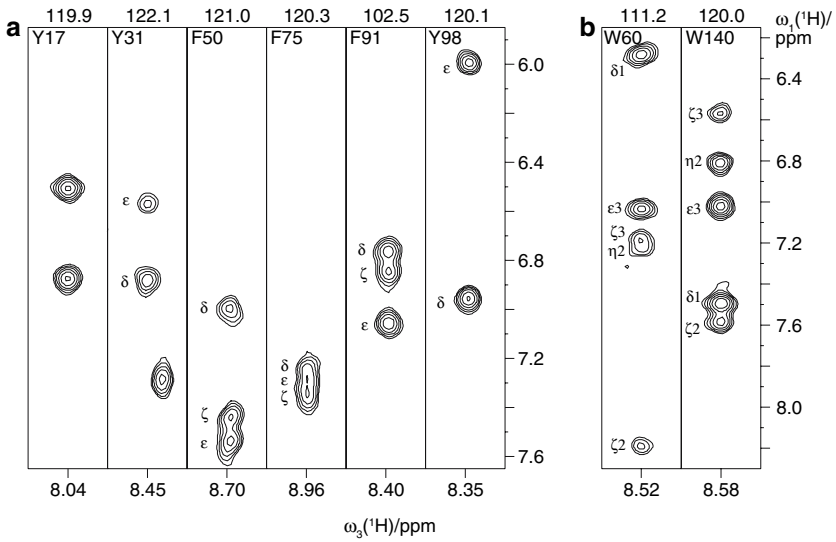

Fig. 7 Unambiguous sequence-specific assignment of aromatic protons in *D. vulgaris* flavodoxin. The $F_1(^{1}H^{ar})$–$F_3(^{1}H^{N})$ strips from (**a**) non-selective and (**b**) Trp-selective 3D H^{ar}(CC-TOCSY-CGCBCACO)NH spectra have widths of 0.25 ppm along F_3, centred around the amide proton chemical shift of the sequentially following residue. The corresponding amide nitrogen chemical shifts along the F_2 dimension are given (in ppm) above each slice

experiments detect histidine $^{13}C^{\beta}$–$^{1}H^{\delta 2}$ correlations in a very sensitive manner (Yamazaki et al. 1993), ε1-protons cannot be assigned because the carbon to which it is attached is separated from the remaining carbons in the imidazole spin system by two nitrogen atoms. Recently we have shown that histidine $\delta 2$ resonances can be directly correlated to backbone amide resonances of the following residue and then, in a second step, linked to the ε1-CH group via one-bond ^{13}C–^{15}N couplings (Löhr et al. 2005). In the following it will be demonstrated that the (H)CB(CGCC-TOCSY)H^{ar} experiment is able to provide sequence-specific $^{1}H^{\varepsilon 1}$ assignments in a single step. To this end the CC-TOCSY mixing time was extended to 44.3 ms (7 cycles of DIPSI-2 at an RF field of 4.5 kHz) resulting in a magnetization transfer through the $^{2}J_{C\gamma C\varepsilon 1}$ coupling. The magnitude of this interaction was measured to be 2.24 ± 0.08 Hz for the three histidine residues in RNase T1 using a [^{13}C, ^{1}H]-TROSY-type (Pervushin et al. 1998, Brutscher et al. 1998) quantitative *J*-correlation (Bax et al. 1994) experiment (F. Löhr, unpublished results). To account for the larger $^{1}J_{CH}$ couplings in the imidazole ring a slightly shorter CP period (4.8 ms at 6 kHz RF field) was employed. Further modifications involve the application of a 3.5-ms C^{γ}-selective REBURP pulse (offset: 133 ppm) in the centre of the $^{1}J_{C\beta C\gamma}$ rephasing delay ζ to prevent evolution of $^{1}J_{C\gamma C\delta 2}$, and the setting of ζ and δ to 9.2 ms and 9.0 ms, respectively. The resulting spectra for RNase T1, flavodoxin and *E.coli* thioredoxin are depicted in Fig. 8. For each histidine residue of these proteins a strong $^{13}C^{\beta}$–$^{1}H^{\delta 2}$ cross peak is accompanied by a significantly weaker correlation to $^{1}H^{\varepsilon 1}$ at the same $^{13}C^{\beta}$ chemical shift making additional experiments for ε1-proton assignments unnecessary.

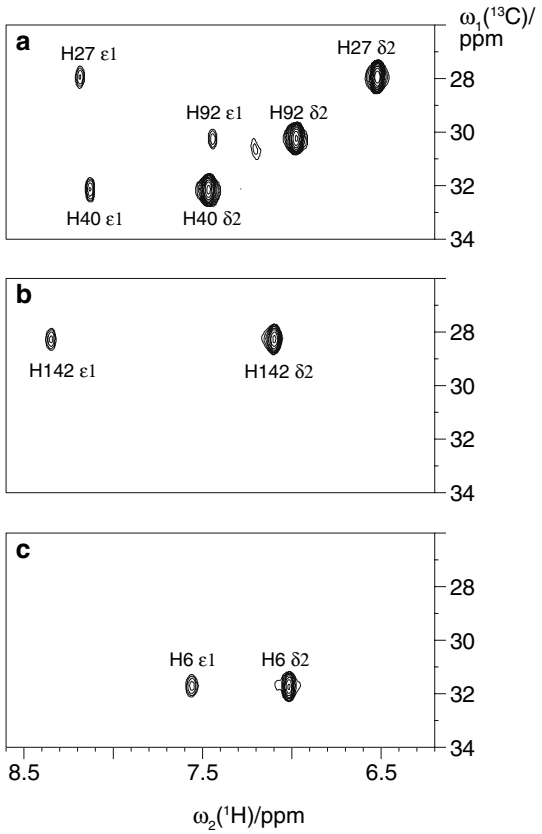

Fig. 8 Regions from (H)CB(CGCC-TOCSY)H^{ar} spectra showing histidine $^{13}C^{\beta}$–$^{1}H^{\delta 2}$ and $^{13}C^{\beta}$–$^{1}H^{\varepsilon 1}$ correlations of (**a**) RNase T1, (**b**) *D. vulgaris* flavodoxin and (**c**) *E.coli* thioredoxin. A CC-TOCSY mixing time of 44.3 ms was employed to achieve a transfer via the two-bond $^{13}C^{\gamma}$–$^{13}C^{\varepsilon 1}$ coupling. The weak unlabelled signal in the spectrum of RNase T1 is due to denatured protein. Proton resonances of thioredoxin are significantly upfield shifted with respect to published chemical shifts (Dyson et al. 1989) because of the higher sample pH in the present study

Complete sequence specific ring proton assignments of all aromatic residues in RNase T1 and flavodoxin, fully consistent with published results (Hoffmann and Rüterjans 1988; Pfeiffer et al. 1996; Knauf et al. 1993, Löhr and Rüterjans 1996), were achieved with the novel (H)CB(CGCC-TOCSY)H^{ar} and H^{ar}(CC-TOCSY-CGCBCACO)NH experiments. Their utility to obtain yet unknown aromatic chemical shifts shall be explored in the following. The emzyme Family-11 xylanase from *Bacillus agaradhaerens*, which catalyses the degradation of xylan, one of the major constituents of plant cell walls (Sabini et al. 1999), consists of 207 amino acid residues (MW 23 kDa) including 13 tyrosines, seven phenylalanines and seven tryptophans. Essentially complete backbone and side-chain assignments including histidine and tryptophan ring resonances have been obtained previously (Betz et al. 2002; Löhr et al. 2002, 2005). Assignment of aromatic tyrosine and phenylalanine protons, however turned out to be challenging. Comparatively fast ^{1}H and ^{13}C transverse relaxation renders through-bond correlation experiments less efficient than for the lower molecular-weight proteins employed in this study and a relatively low sample concentration (0.5 mM) additionally decreased sensitivity. Moreover, degradation products in the five-year old xylanase sample deteriorated spectra quality in $^{13}C^{\beta}$–$^{1}H^{ar}$ correlated experiments while extensive overlap of $^{13}C^{\beta}$ resonance frequencies complicated assignments.

From (Hβ)Cβ(CγCδ)Hδ (Fig. 9a) and (Hβ)Cβ(CγCδCε)Hε (Fig. 9b) spectra of xylanase unequivocal assignments were only obtained for Tyr144, Phe163 and Tyr195, which have unique $^{13}C^{\beta}$ chemical shifts. A very weak correlation was observed for the Phe163 $^{1}H^{\varepsilon}$ resonance in the (Hβ)Cβ(CγCδCε)Hε while the

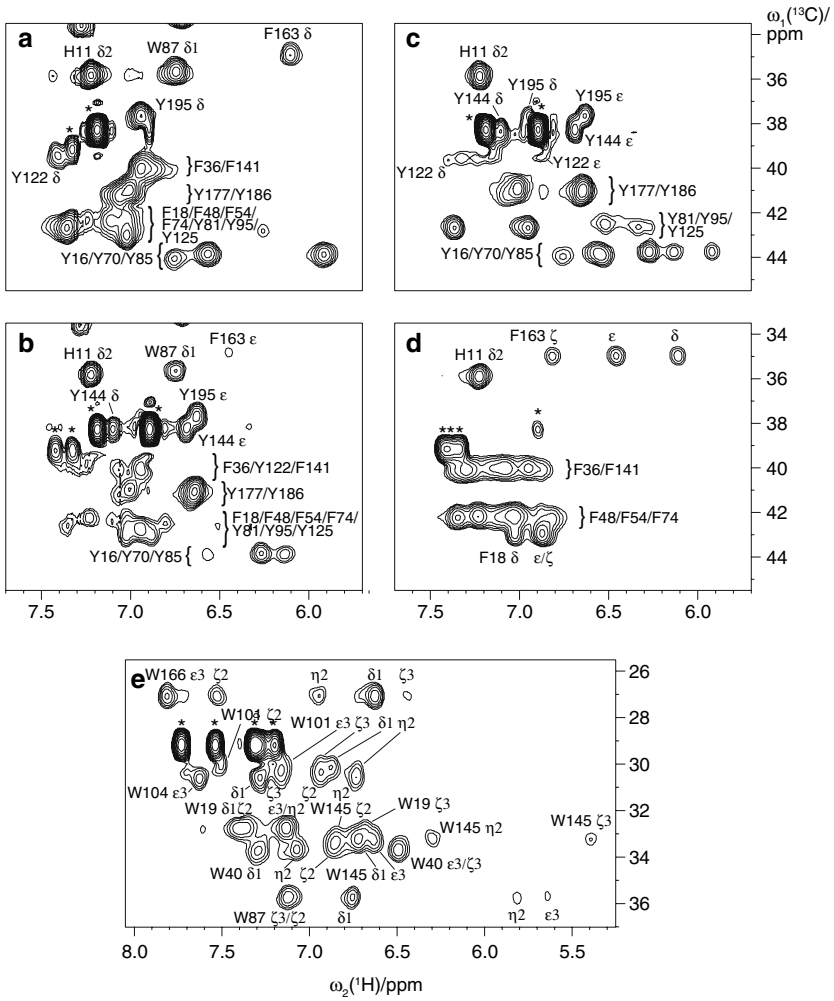

Fig. 9 Application of (**a**) (Hβ)Cβ(CγCδ)Hδ, (**b**) (Hβ)Cβ(CγCδCε)Hε, (**c**) Tyr-selective (H)CB(CGCC-TOCSY)H^{ar}, (**d**) Phe-selective (H)CB(CGCC-TOCSY)H^{ar} and (**e**) Trp-selective (H)CB(CGCC-TOCSY)H^{ar} pulse sequences to xylanase from *Bacillus agaradhaerens*. All spectra were recorded and processed identically and contour lines in plots (**a–d**) are drawn at the same levels. Cross peask arising from degradation products are labelled with asterisks. Braces indicate regions where individual aromatic residues cannot be distinguished due to near-degenerate $^{13}C^{\beta}$ chemical shifts. Tryptophan ring protons have been assigned previously using other methods (Löhr et al. 2002, 2005). A cross peak of His11 is observed in both Tyr- and Phe-selective (H)CB(CGCC-TOCSY)H^{ar} experiments because, at the present pH, its γ-carbon resonates at 135.5 ppm (Betz et al. 2004), approximately midway between the positions of the $^{13}C^{\gamma}$-selective refocusing pulses in the respective pulse sequences

(Hβ)Cβ(Cγ CδCε Cζ)Hζ (not shown) exclusively contained cross peaks belonging to degradation products. In contrast, all three aromatic proton resonances are readily detected in the Phe-selective (H)CB(CGCC-TOCSY)H^{ar} experiment (Fig. 9d). The Tyr-selective (H)CB(CGCC-TOCSY)H^{ar} spectrum (Fig. 9c) permits assignment of the Tyr195 $^{1}H^{\varepsilon}$ resonance but the corresponding $^{13}C^{\beta}$–$^{1}H^{\delta}$ correlation is obscured by a very intense signal due to a tyrosine-containing peptide fragment. The use of amino-acid type selective (H)CB(CGCC-TOCSY)H^{ar} versions simplifies spectra to some extent but, with the exception of Phe18, which can thus be distinguished from Tyr81, Tyr95 and Tyr125, $^{13}C^{\beta}$ chemical shifts of the remaining tyrosine and phenylalanine residues of xylanase are almost degenerate with those of at least one other aromatic amino acid preventing sequence specific assignment of ring protons. This also applies to the Trp-selective version shown in Fig. 9e. Although all were detected, several indole protons cannot be clearly identified because of severe overlap between the spin systems of Trp19/Trp40/Trp145 and of Trp101/Trp104 and a tryptophan-containing degradation product.

The potential of the H^{ar}(CC-TOCSY-CGCBCAC-O)NH sequence to resolve signal overlap encountered in $^{13}C^{\beta}$–$^{1}H^{\delta}$ correlated spectra of xylanase in demonstrated in Fig. 10. Each of the three amino-acid type selective 2D (H^{ar}CC-TOCSY-CGCBCACO)NH spectra, which correspond to projections of a 3D spectrum on the ^{15}N–$^{1}H^{N}$ plane, show well-dispersed cross peaks with little interference from degradation products. The only exception is found in Fig. 10a, where cross peaks from Tyr16 and Tyr122 nearly coincide. Signals are detected for all phenylalanine and tryptophan residues and ten out of 13 tyrosine residues. Two of the remaining three tyrosines are likewise unobservable in either (Hβ)Cβ(CγCδ)Hδ or (H)CB(CGCC-TOCSY)H^{ar} experiments. No signal originating from non-aromatic residues is seen in any of the spectra and there is no 'cross-talk' between the three selected

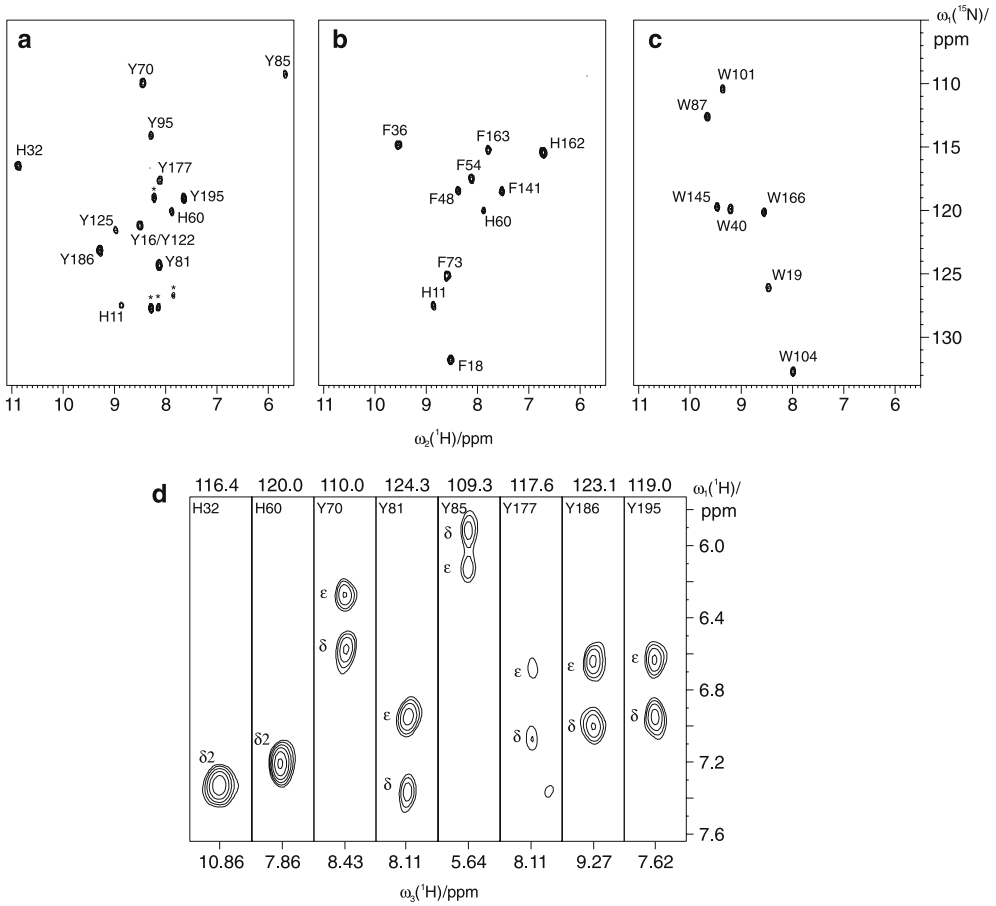

Fig. 10 Two-dimensional (**a**) Tyr-, (**b**) Phe- and (**c**) Trp-selective (H^{ar}CC-TOCSY-CGCBCACO)NH spectra and (d) expansions of F_1–F_3($^1H^{ar}$–$^1H^N$) slices from a three-dimensional H^{ar}(CC-TOCSY-CGCBCACO)NH spectrum of xylanase. Peaks are labelled with the residue number preceding the one whose amide ^{15}N and ^1H chemical shifts are detected. The F_1–F_3 strips of panel d have a width of 0.3 ppm along F_3 and are taken at the ^{15}N (F_2) chemical shifts indicated above each slice. Asterisks denote cross peaks due to degradation products

residue types. Therefore, such 2D amino-acid type selective ^{15}N–$^1H^N$ correlations may provide valuable information at the early stages of the sequential backbone assignment process (Schubert et al. 2001). Note, however, that cross peaks due to histidine residues may appear in either Tyr- or Phe-selective spectra or both (e.g., His11), depending on their $^{13}C^{\gamma}$ chemical shift. Usually they are readily identified in the three-dimensional version, giving rise to a single correlation with the $\delta 2$-proton. Taking a 3D Tyr-selective H^{ar}(CC-TOCSY-CGCBCACO)NH spectrum as an example, Fig. 10d shows the actual assignment ring protons of xylanase. In most cases unambiguous sequence specific assignments are readily obtained. On the other hand, despite an extended period of measurement time (5.5 days) employed here, some cross peaks are rather weak (e.g., Y85, Y177), indicating that efficient application of 3D H^{ar}(CC-TOCSY-CGCBCACO)NH experiments is limited to relatively small proteins with molecular weights below ≈20 kDa.

Apart from relaxation, low intensities or even absence of signals in H^{ar}(CC-TOCSY-CGCBCACO)NH spectra may be a consequence of fast amide proton exchange with the solvent. A possible way to circumvent this difficulty while still benefitting from the superior spectral dispersion of backbone nuclei, is the carbonyl detected HC^{ar}(CC-TOCSY-CGCBCA)-CO experiment. Advantages of carbonyl versus α-carbon detection are the comparatively long transverse relaxation times at moderate static magnetic fields and the straightforward removal of splittings due to homonuclear couplings using a simple IPAP module. Unlike 'protonless' experiments (Bermel et al. 2006) the sequence exploits ^1H polarization via an initial INEPT transfer step, considerably enhancing sensitivity for diamagnetic proteins. The total duration of ^1H transverse magnetization is limited to the length of the t_1 evolution time, possibly enabling application to aromatic residues subject to moderate paramagnetic line broadening. Obviously, direct excitation of carbon spins is not an option because the primary aim of the experiment is the assignment of aromatic protons. Aromatic ^{13}C chemical shifts are nevertheless sampled in the course of the INEPT sequence by semi-constant time t_2 evolution.

The result of a non-selective 3D HC^{ar}(CC-TOCSY-CGCBCA)CO experiment applied to RNase T1 is presented in Fig. 11. Using a CC-TOCSY mixing time

of 8 ms, approximately equal cross peak intensities are observed for δ- and ε-positions of tyrosines. Thanks to the aromatic ^{13}C chemical shift labelling along the F_2 dimension signals are well dispersed, confirming that the detection of only one cross peak for Tyr57 in the (H)CB(CGCC-TOCSY)H^{ar} spectra of Fig. 5 is due to a degeneracy of $^1H^{\delta}$ and $^1H^{\varepsilon}$ chemical shifts. For histidine and tryptophan spin systems correlations only involve δ-CH groups at the mixing time chosen here. Note that no information about Trp59 would be obtained in the proton-detected H^{ar}(CC-TOCSY-CGCBCACO)NH experiment of RNase T1 because this residue is sequentially followed by a proline. Signal intensities in phenylalanine rings significantly decrease in the order $\delta > \varepsilon > \zeta$. We were unable to find a TOCSY spin-lock time suitable to obtain uniform intensities for both tyrosine and phenylalanine spin systems, recalling that the heteronuclear cross-polarization period in (H)CB(CGCC-TOCSY)H^{ar} and H^{ar}(CC-TOCSY-CGCBCACO)NH experiment, which is missing here, also contributes to homonuclear mixing. Separate HC^{ar}(CC-TOCSY-CGCBCA)CO experiments optimized for phenylalanine and tryptophan residues were therefore performed using mixing times of 11.1 ms and 15 ms, respectively. Figure 12 shows F_1–F_2 slices of the corresponding amino-acid type selective spectra of oxidized *E. coli* thioredoxin resulting in full aromatic resonance assignments for each of its four phenylalanine and both tryptophan residues. Proton chemical shifts are in accord with those observed by Dyson et al. (1989) while ^{13}C assignments were previously unpublished. Once again, an ambiguity encountered in the (H)CB(CGCC-TOCSY)H^{ar} spectrum (not shown) caused by near-degeneracy of $^1H^{\zeta 2}$ and $^1H^{\varepsilon 3}$ resonances of Trp31 is lifted owing to their separation along the $^{13}C^{ar}$ dimension.

The carbon-detected experiments presented in Fig. 11 and 12 were less sensitive than corresponding proton-detected experiments carried on the same samples by, roughly, an order of magnitude. This implies that use of the HC^{ar}(CC-TOCSY-CGCBCA)-CO sequence requires favourable sample conditions (relatively high sample concentrations and temperature, narrow ^{13}C lines). A wider range of applications is however conceivable when cryogenic probes optimized for ^{13}C detection are available.

Conclusions

Based on the widely used (Hβ)Cβ(CγCδ)Hδ/(Hβ)Cβ(CγCδCε)Hε pulse sequence pair a novel through-bond correlation scheme named (H)CB(CGCC-TOCSY)H^{ar} has been developed to obtain sequence-specific resonance assignments of aromatic protons. Because aromatic CC-COSY and CH-INEPT steps are avoided the sequence it is not affected by strong ^{13}C–^{13}C coupling, and detrimental conformational exchange effects caused by ring flips on

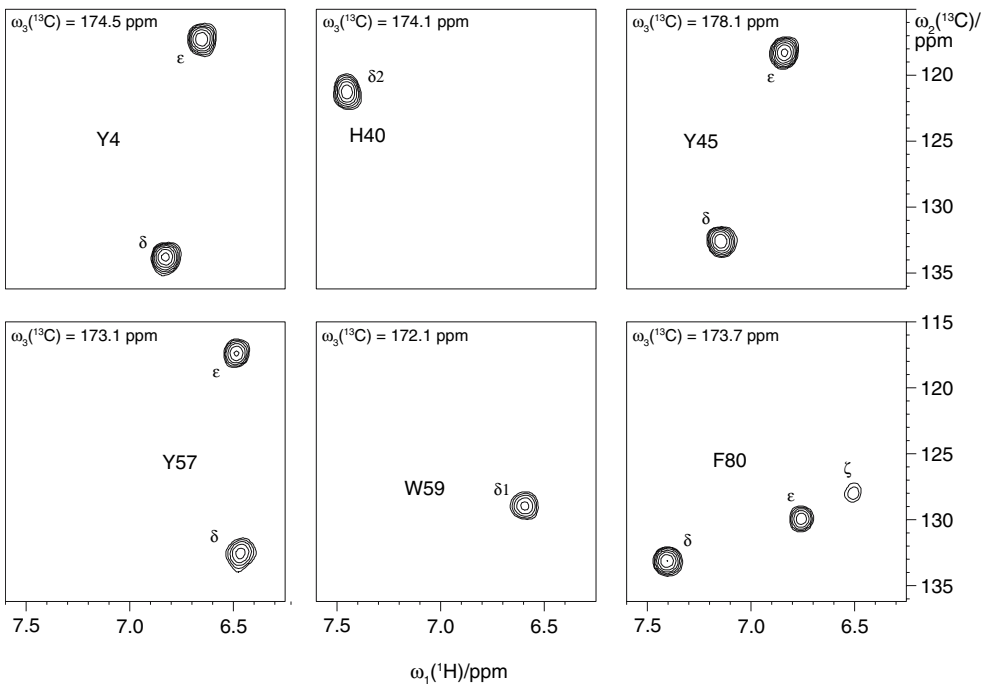

Fig. 11 Intraresidual correlations between carbonyl carbons and aromatic protons/carbons in RNase T1. Shown are F_1–F_2 planes are extracted from a ^{13}C-detected, non-selective 3D HC^{ar}(CC-TOCSY-CGCBCA)CO spectrum at the ^{13}C′ (F_3) chemical shifts indicated in the upper left corner of each slice

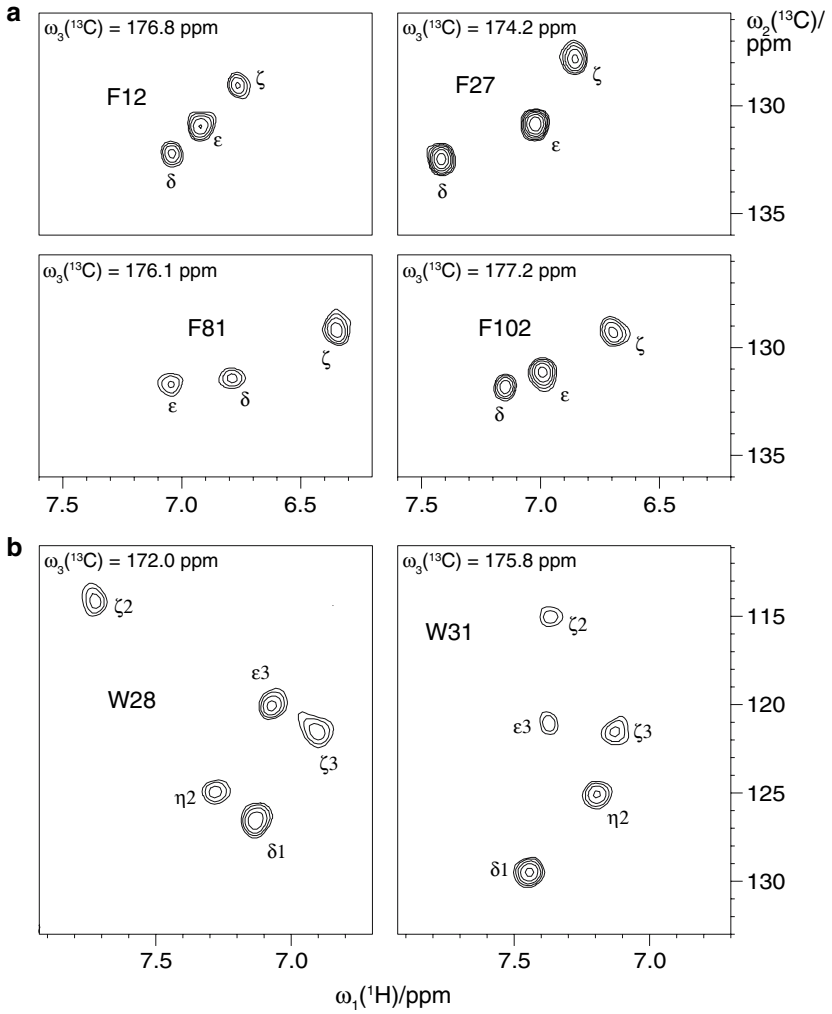

Fig. 12 Assignment of aromatic proton and carbon resonances of *E.coli* thrioredoxin. Slices are taken from (**a**) Phe- and (**b**) Trp-selective 3D HC^{ar}(CC-TOCSY-CGCBCA)CO spectra recorded with CC-TOCSY mixing times of 11.1 ms and 15.0 ms, respectively

an intermediate time scale are minimized. This allows efficient magnetization transfer via scalar couplings up to the ζ-CH position in phenylalanine side chains. Optionally, amino-acid type selective versions can by applied to disentangle phenylalanine and tyrosine cross peak patterns which share the same $^{13}C^{\beta}$ chemical shift range, a welcome side effect being increased sensitivity. Connectivities between β-carbons and protons of the benzene moiety of the indole ring system in tryptophan side chains or ε1-protons in histidine side chains become accessible when elongated CC-TOCSY mixing periods are employed. Application of the Trp-selective version avoids difficulties due to the presence of very strong histidine $^{13}C^{\beta}$–$^{1}H^{\delta}$ signals in non-selective spectra of His-tagged proteins, often concealing correlations from tryptophan residues in the same region.

In the case of yet unknown $^{13}C^{\beta}$ assignments or excessive resonance overlap, aromatic chemical shifts may be directly linked to the protein backbone using either ^{1}H-detected H^{ar}(CC-TOCSY-CGCBCAC-O)NH or ^{13}C-detected HC^{ar}(CC-TOCSY-CGCBCA)-CO techniques. Despite its numerous coherence transfer steps the former scheme has been demonstrated to yield excellent sensitivity for a 16-kDa protein and afforded unambiguous and complete $^{1}H^{ar}$ assignments that were difficult to obtain be other means. Being substantially prone to transverse relaxation its efficiency, however, rapidly decreases with increasing rotational correlation time of the protein under investigation. Transverse relaxation is somewhat less critical in the latter version, which is shorter, but suffers from an unavoidable loss of sensitivity due to direct carbon detection. Nevertheless, it can be expected to be a useful alternative when amide protons are not observable or have a very low dispersion as, for example, in unfolded proteins. Moreover, additional sampling of aromatic carbon chemical shifts in the HC^{ar}(CC-TOCSY-CGCBCA)CO experiment helps to obtain regioselective assignments in tyrosine and

tryptophan side chains and facilitates subsequent analysis of ^{13}C-edited NOESY spectra.

Acknowledgements The authors would like to thank Gary Yalloway and Christian Klammt for the preparation of *D. vulgaris* flavodoxin. The samples of RNase T1 and xylanase were kindly provided by Norman Spitzner and Marco Betz, respectively. Recombinant xylanase was produced in collaboration with Novo-Nordisk A/S (Bagsvaerd, Denmark). Financial support from the Deutsche Forschungsgemeinschaft (BE 1911/4) is gratefully acknowledged. The Centre for Biomolecular Magnetic Resonance is supported by the state of Hesse.

References

AB E, Pugh DJR, Kaptein R, Boelens R, Bonvin AMJJ (2006) Direct use of unassigned resonances in NMR structure calculations with proxy residues. J Am Chem Soc 128:7566–7571

Andersson P, Weigelt J, Otting G (1998) Spin-state selection filters for the measurement of heteronuclear one-bond coupling constants. J Biomol NMR 12:435–441

Babini E, Bertini I, Capozzi F, Felli IC, Lelli M, Luchinat C (2004) Direct carbon detection in paramagnetic metalloproteins to further exploit pseudocontact shift restraints. J Am Chem Soc 126:10496–10497

Bax A, Clore GM, Gronenborn AM (1990) ^{1}H-^{1}H correlation via isotropic mixing of ^{13}C magnetization, a new three-dimensional approach for assigning ^{1}H and ^{13}C spectra of ^{13}C-enriched proteins. J Magn Reson 88:425–431

Bax A, Vuister GW, Grzesiek S, Delaglio F, Wang AC, Tschudin R, Zhu G (1994) Measurement of homo-and heteronuclear *J* couplings from quantitative *J* correlation. In: James TL, Oppenheimer NJ (eds) Methods in enzymology, vol 239. Academic Press, New York, pp 79–105

Bearden DW, Brown LR (1989) Heteronuclear isotropic mixing in liquids. Chem Phys Lett 163:432–436

Bermel W, Bertini I, Duma L, Felli IC, Emsley L, Pierattelli R, Vasos PR (2005) Complete assignment of heteronuclear protein resonances by protonless NMR spectroscopy. Angew Chem Int Ed Engl 44:3089–3092

Bermel W, Bertini I, Felli IC, Kümmerle R, Pierattelli R (2003) ^{13}C direct detection experiments in the paramagnetic oxidized monomeric copper, zinc superoxide dismutase. J Am Chem Soc 125:16423–16429

Bermel W, Bertini I, Felli IC, Piccioli M, Pierattelli R (2006) ^{13}C-detected protonless NMR spectroscopy of proteins in solution. Prog Nucl Magn Res Spectrocs 48:25–45

Bertini I, Felli IC, Kümmerle R, Luchinat C, Pierattelli R (2004a) ^{13}C–^{13}C NOESY: A constructive use of ^{13}C–^{13}C spin diffusion. J Biomol NMR 30:245–251

Bertini I, Duma L, Felli IC, Fey M, Luchinat C, Pierattelli R, Vasos PR (2004b) A heteronuclear direct-detection NMR spectroscopy experiment for protein-backbone assignment. Angew Chem Int Ed Eng 43:2257–2259

Bertini I, Lee Y-M, Luchinat C, Piccioli M, Poggi L (2001) Locating the metal ion in calcium-binding proteins by using cerium(III) as a probe. Chem Bio Chem 2:550–558

Betz M, Löhr F, Wienk H, Rüterjans H (2002) Letter to the Editor: ^{1}H, ^{13}C and ^{15}N chemical shifts assignment of *Bacillus agaradhaerens* family 11 xylanase. J Biomol NMR 23:333–334

Betz M, Löhr F, Wienk H, Rüterjans H (2004) Long-range nature if the interactions between titratable groups in *Bacillus agaradhaerens* family 11 xylanase: pH titration of *B. agaradhaerens* xylanase. Biochemistry 43: 5820–5831

Billeter M, Braun W, Wüthrich K (1982) Sequential resonance assignments in protein ^{1}H nuclear magnetic resonance spectra. Computation of sterically allowed proton-proton distances and statistical analysis of proton-proton distances in single crystal protein conformations. J Mol Biol 155:321–346

Boyd J, Soffe N (1989) Selective excitation by pulse shaping combined with phase modulation. J Magn Reson 85:406–413

Brutscher B, Boisbouvier J, Pardi A, Marion D, Simorre J-P (1998) Improved sensitivity and resolution in ^{1}H–^{13}C NMR experiments of RNA. J Am Chem Soc 120:11845–11851

Burum DP, Ernst RR (1980) Net polarization transfer via a *J*-ordered state for signal enhancement of low-sensitivity nuclei. J Magn Reson 39:163–168

Cavanagh J, Palmer III AG, Wright PE, Rance M (1991) Sensitivity improvement in proton-detected two-dimensional heteronuclear relay spectroscopy. J Magn Reson 91:429–436

Carlomagno T, Maurer M, Sattler M, Schwendinger MG, Glaser SJ, Griesinger C (1996) PLUSH TACSY: homonuclear planar TACSY with two-band selective shaped pulses applied to C^{α},C' transfer and C^{β},$C^{aromatic}$ correlations. J Biomol NMR 8:161–170

Curley GP, Carr MC, Mayhew SG, Voordouw G (1991) Redox and flavin-binding properties of recombinant flavodoxin from *Desulfovibrio vulgaris* (Hildenborough). Eur J Biochem 202:1091–1100

Dyson HJ, Holmgren A, Wright PE (1989) Assignment of the proton NMR spectrum of reduced and oxidized thioredoxin: sequence-specific assignments, secondary structure, and global fold. Biochemistry 28:7074–7087

Eletsky A, Moreira O, Kovacs H, Pervushin K (2003) A novel strategy for the assignment of side-chain resonances in completely deuterated large proteins using ^{13}C spectroscopy. J Biomol NMR 26:167–179

Emsley L, Bodenhausen G (1990) Gaussian pulse cascades: new analytical functions for rectangular selective inversion and in-phase excitation in NMR. Chem Phys Lett 165:469–476

Ernst M, Griesinger C, Ernst RR, Bermel W (1991) Optimized heteronuclear cross polarization in liquids. Mol Phys 74:219–252

Fesik SW, Eaton HL, Olejniczak ET, Zuiderweg ERP, McIntosh LP, Dahlquist FW (1990) 2D and 3D NMR spectrocopy employing ^{13}C–^{13}C magnetization transfer by isotropic mixing. Spin system identification in large proteins. J Am Chem Soc 112:886–888

Geen H, Freeman R (1991) Band-selective radiofrequency pulses. J Magn Reson 93:93–141

Grzesiek S, Anglister J, Bax A (1993) Correlation of backbone amide and aliphatic side-chain resonances in ^{13}C/^{15}N-enriched proteins by isotropic mixing of ^{13}C magnetization. J Magn Reson B101:114–119

Grzesiek S, Bax A (1992) Correlating backbone amide and side chain resonances in larger proteins by multiple relayed triple resonance NMR. J Am Chem Soc 114:6291–6293

Grzesiek S, Bax A (1993) Amino acid type determination in the sequential assignment procedure of uniformly ^{13}C/^{15}N-enriched proteins. J Biomol NMR 3:185–204

Grzesiek S, Bax A (1995) Audio-frequency NMR in a nutating frame. Application to the assignment of phenylalanine residues in isotopically enriched proteins. J Am Chem Soc 117:6527–6531

Hoffmann E, Rüterjans H (1988) Two-dimensional ^{1}H-NMR investigation of ribonuclease T_1. Resonance assignments, secondary and low-resolution structures of ribonuclease T_1. Eur J Biochem 177:539–560

Kay LE, Keifer P, Saarinen T (1992) Pure absorption gradient enhanced heteronuclear single quantum correlation spectroscopy with improved sensitivity. J Am Chem Soc 114:10663–10665

Knauf M, Löhr F, Curley GP, O'Farrell P, Mayhew SG, Müller F, Rüterjans H (1993) Homonuclear and heteronuclear NMR studies of oxidized *Desulfovibrio vulgaris* flavodoxin. Sequential assignments and identification of secondary structure elements. Eur J Biochem 213:167–184

Kostic M, Pochapsky SS, Pochapsky TC (2002) Rapid recycle ^{13}C', ^{15}N and ^{13}C,^{13}C' heteronuclear and homonuclear multiple quantum coherence detection for resonance assignments in paramagnetic proteins: Example of Ni^{2+}-containing acireductone dioxygenase. J Am Chem Soc 124:9054–9055

Kupče Ë, Freeman R (1995) Adiabatic pules for wideband inversion and broadband decoupling. J Magn Reson A115:273–276

Lin Z, Xu Y, Yang S, Yang D (2006) sequence-specific assignment of aromatic resonances of uniformly ^{13}C,^{15}N-labeled proteins by using ^{13}C- and ^{15}N-edited NOESY spectra. Angew Chem Int Ed Eng 45:1960–1963

Logan TM, Olejniczak ET, Xu RX, Fesik SW (1992) Side chain and backbone assignments in isotopically labeled proteins from two heteronuclear triple resonance experiments. FEBS Lett 314:413–418

Logan TM, Olejniczak ET, Xu RX, Fesik SW (1993) A general method for assigning NMR spectra of denatured proteins using 3D HC(CO)NH-TOCSY triple resonance experiments. J Biomol NMR 3:225–231

Löhr F, Rüterjans H (1996) Novel pulse sequences for the resonance assignment of aromatic side chains in ^{13}C-labeled proteins. J Magn Reson B112:259–268

Löhr F, Katsemi V, Betz M, Hartleib J, Rüterjans H (2002) Sequence-specific assignment of histidine and tryptophan ring ^{1}H, ^{13}C and ^{15}N resonances in ^{13}C/^{15}N- and ^{2}H/^{13}C/^{15}N-labelled proteins. J Biomol NMR 22:153–164

Löhr F, Rogov VV Shi M, Bernhard F, Dötsch V (2005) Triple-resonance methods for complete resonance assignment of aromatic protons and directly bound heteronuclei in histidine and tryptophan residues. J Biomol NMR 32:309–328

Machonkin TE, Westler WM, Markley JL (2002) ^{13}C{^{13}C} 2D NMR: a novel strategy for the study of paramagnetic proteins with slow electronic relaxation rates. J Am Chem Soc 124:3204–3205

Machonkin TE, Westler WM, Markley JL (2004) Strategy for the study of paramagnetic proteins with slow electronic relaxation rates by NMR spectrocopy: application to oxidized human [2Fe-2S] ferredoxin. J Am Chem Soc 126:5413–5426

Marion D, Ikura M, Tschudin R, Bax A (1989) Rapid recording of 2D NMR spectra without phase cycling. Application to the study of hydrogen exchange in proteins. J Magn Reson 85:393–399

Montelione GT, Lyons BA, Emerson SD, Tashiro M (1992) An efficient triple resonance experiment using carbon-13 isotropic mixing for determining sequence-specific resonance assignments of isotopically-enriched proteins. J Am Chem Soc 114:10974–10975

Muhandiram DR, Kay LE (1994) Gradient-enhanced triple-resonance three-dimensional NMR experiments with improved sensitivity. J Magn Reson B103:203–216

Nielsen NC, Thøgersen H, Sørensen OW (1995) Doubling the sensitivity of INADEQUATE for tracing out the carbon skeleton of molecules by NMR. J Am Chem Soc 117:11365–11366

Oh BH, Westler WM, Darba P, Markley JL (1988) Protein carbon-13 spin systems by a single two-dimensional nuclear magnetic resonance experiment. Science 240:908–911

Ottiger M, Delaglio F, Bax A (1998) Measurement of *J* and dipolar couplings from simplified two-dimensional NMR spectra. J Magn Reson 131:373–378

Patt S (1992) Single- and multiple-frequency-shifted laminar pulses. J Magn Reson 96:94–102

Pervushin K, Riek R, Wider G, Wüthrich K (1998) Transverse relaxation-optimized spectroscopy (TROSY) for NMR studies of aromatic spin systems in ^{13}C-labeled proteins. J Am Chem Soc 120:6394–6400

Pervushin K, Eletsky A (2003) A new strategy for backbone resonance assignment in large proteins using a MQ-HAC-ACO experiment. J Biomol NMR 25:147–152

Peti W, Norcross J, Eldridge G, O'Neill-Johnson M (2004) Biomolecular NMR using a microcoil NMR probe – New technique for the chemical shift assignment of aromatic side chains in proteins. J Am Chem Soc 126:5873–5878

Pfeiffer S, Engelke J, Rüterjans H (1996) Complete ^{1}H, ^{15}N and ^{13}C resonance assignment of ribonuclease T_1: Secondary structure and backbone dynamics as derived from the chemical shifts. Quart Magn Res Biol Med 3:69–87

Prompers JJ, Groenewegen A, Hilbers CW, Pepermans HAM (1998) Two-dimensional NMR experiments for the assignment of aromatic side chains in ^{13}C-labeled proteins. J Magn Reson 130:68–75

Sabini E, Sulzenbacher G, Dauter M, Dauter Z, Jorgensen PL, Schulein M, Dupont C, Davies GJ, Wilson KS (1999) Catalysis and specificity in enzymatic glycoside hydrolysis: a 2,5B conformation for the glycosyl-enzyme intermediate revealed by the structure of the *Bacillus agaradhaerens* family 11 xylanase. Chem Biol 6:483–492

Schlörb C, Ackermann K, Richter C, Wirmer J, Schwalbe H (2005) Heterologous expression of hen egg white lysozyme and resonance assignment of tryptophan side chains in ist non-native states. J Biomol NMR 33:95–104

Schubert M, Schmieder P, Oschkinat H (2001) MUSIC and aromatic residues: amino acid type-selective ^{1}H- ^{15}N correlations, III. J Magn Reson 153:186–192

Serber Z, Richter C, Dötsch V (2001) Carbon-detected NMR experiments to investigate structure and dynamics of biological macromolecules. Chem Bio Chem 2:247–251

Shaka AJ, Barker PB, Freeman R (1985) Computer-optimized decoupling scheme for wideband applications and low-level operation. J Magn Reson 64:547–552

Shaka AJ, Keeler J, Frenkiel T, Freeman R (1983) An improved sequence for broadband decoupling: WALTZ-16. J Magn Reson 52:335–338

Shaka AJ, Lee CJ, Pines A (1988) Iterative schemes for bilinear operators; application to spin decoupling. J Magn Reson 77:274–293

Spitzner N, Löhr F, Pfeiffer S, Koumanov A, Karshikoff A, Rüterjans H (2001) Ionization properties of titratable groups in ribonuclease T_1.I.pK_a values in the native state determined by two-dimensional heteronuclear NMR spectrocopy. Eur Biophys J 30:186–197

Torizawa T, Mei Ono A, Terauchi T, Kainosho M (2005) NMR assignment methods for the aromatic ring resonances of phenylalanine and tyrosine residues in proteins. J Am Chem Soc 127:12620–12626

Wagner G, Wüthrich K (1982) Sequential resonance assignments in protein ^{1}H nuclear magnetic resonance spectra. Basic pancreatic trypsin inhibitor. J Mol Biol 155:347–366

Wüthrich K (1986) NMR of proteins and nucleic acids. Wiley, New York NY

Yamazaki T, Forman-Kay JD, Kay LE (1993) Two-dimensional NMR experiments for correlating $^{13}C\beta$ and $^{1}H\delta/\varepsilon$ chemical shifts of aromatic residues in ^{13}C-labeled proteins via scalar couplings. J Am Chem Soc 115:11054–11055

Zuiderweg ERP (1990) Analysis of multiple-pulse-based heteronuclear *J* cross polarization in liquid. J Magn Reson 89:533–542